Rochester Institute of Technology
RIT Digital Institutional Repository

Theses

2-1-1994

Plasma modification of poly(ester sulfonic) acid aniomoneric membranes

Linda Slapelis

Follow this and additional works at: https://repository.rit.edu/theses

Recommended Citation
Slapelis, Linda, "Plasma modification of poly(ester sulfonic) acid aniomoneric membranes" (1994). Thesis. Rochester Institute of Technology. Accessed from

This Thesis is brought to you for free and open access by the RIT Libraries. For more information, please contact repository@rit.edu.

Plasma Modification of Poly(ester sulfonic) Acid Anionomeric Membranes

Linda Slapelis

Thesis
Submitted in partial fulfillment of the requirements for the degree of
Master of Science

February, 1994

Approved:

Dr. Thomas Gennett Thesis Advisor	Dr. Merle Hirsh Thesis Advisor
Dr. Mike Jackson Thesis Committee	Dr. Andreas Langner Thesis Committee
Library	

Rochester Institute of Technology
Rochester, New York 14623
Center of Materials Science and Engineering

Plasma Modification of Poly(ester sulfonic) Acid Anionomeric Membranes

I, Linda Slapelis, hereby grant permission to the Wallace Library of the Rochester Institute of Technology to maintain a copy and to reproduce my thesis in whole or in part. Any reproduction will not be for commercial use or profit.

_____ date: May, 1994

Linda Slapelis

Abstract

The effect of variations in plasma parameters on the fluorination, degradation, and etching of poly(ester sulfonic) acid (AQ55) anionomeric membranes was examined. The determination of how the plasma gas composition, power, proximity of the sample to the glow, and time of exposure could be used to maximize surface fluorination and minimize degradation of polymer films is discussed. Membrane surfaces were characterized using contact angles, SEM, gravimetric analysis, DSC, FTIR/MIR, and XPS. These techniques aided in the determination of changes in surface energy, surface topography, sample weight, bulk property, and the identification and quantification of chemical functionalities produced at the AQ55 surface after plasma modification. For all plasma treatments, a range of 9% to 60% atomic fluorine was detected within a depth of 50 Å. The degree of fluorination was enhanced by limiting the effects of surface etching and degradation. Three factors which were found to promote surface degradation and etching included; the presence of oxygen, high energy ion bombardment, and elevated plasma temperatures. Under these conditions, the effects of degradation and etching were increased with time of exposure.

Gas mixtures of 5% O_2/10% Ar/85% CF_4 and 10% Ar/90% CF_4 were used to ascertain the type and degree of modification produced with and without the presence of oxygen. An increase in the power from 20 W to 50 W increased plasma-surface interactions which resulted in an increase of 10% atomic fluorine at the surface. The effects of ion bombardment were reduced by suspending a quartz plate over the samples during plasma modification. This proved to double the percent atomic fluorine and eliminate degradation and/or etching at the AQ55 surface.

The parameters which were found to maximize fluorination and minimize surface degradation and etching include: a 10% Ar/90% CF_4 gas composition, 50 W power, long exposure times, and use of the quartz plate shield. Under these conditions, the percent atomic carbon, oxygen and fluorine detected on the surface changed from 74% C, 26% O, 0% F, to 36% C, 4% O, and 60% F.

Table of Contents

List of Figures

List of Tables

Acknowledgments

I would like to sincerely thank my research advisors Dr. Tom Gennett and Dr. Merle Hirsh for their continued assistance, guidance and most of all, their patience in completing this Maters thesis project. The completion of this project would not have been possible without the additional help and expertise of the following people: Dr. Gerald Takacs, Dr. Andreas Langner, Dr. Mike Jackson, Dr. Tom Debies, Dr. Luiz Matienzo, Dr. Frank Egitto, Ken Kemp, Xiarong Lin, and T. Edwin Freeman.

I would like to thank Dr. Takacs for his assistance and keeping his door open to answer many of my questions. Many thanks goes to Dr. Langner for his dedication and devotion in teaching Polymer Science. Many thanks also goes to Dr. Mike Jackson for the supply of silicon wafers, his help in the Microelectronic Engineering clean room, and with the SEM analysis.

I would like to acknowledge and thank Dr. Luiz Matienzo and Dr. Frank Egitto from IBM Corp. for the XPS analysis and the discussions about plasma modification of polymers. Many, many thanks also goes to Dr. Tom Debies and Ken Kemp from Xerox Corp. for the contribution of numerous XPS and SEM analyses.

Finally, a very special thanks goes to Xiarong Lin and T. Edwin Freeman for their support and friendship during my stay at RIT. Their help will be remembered and appreciated.

Dedication

To my parents, Vito and Marie

Thank you!
Without your love and support this would have been impossible.

1.0. Introduction

Plasma modification of polymeric materials has been the subject of considerable research in recent years. Investigations on polymer surface modifications produced by a plasma have included: etching, polymerization, alterations in hydrophobicity/hydrophilicity, surface biocompatibility, adhesion, and surface fluorination. Plasma processes are progressively replacing other methods of surface modification because they are dry, clean processes that do not alter the already favorable bulk properties of a material.

Surface fluorination of hydrocarbon polymers by a plasma process has gained the attention of researchers since the mid 1960's.[1-12] Through plasma fluorination, low intermolecular dispersion forces have been generated at the polymer surface to produce a chemically resistant surface.[1-12] The presence of fluorocarbon functionalities in a polymer structure imparts extreme hydrophobicity, water insolubility, higher thermal and oxidative stabilities and chemical resistance. Also, interactions between C-F bonds of adjacent polymer chains may be so strong that the polymer will not dissolve in any solvent. Such a protective surface is quite desirable for a wide range of applications. Specific investigations of plasma fluorination of polymers have included surface fluorination of polyethylene,[1-5,7] polystyrene,[5,8] polyimide,[9,10,12] polypropylene,[6,7] and lignocellulose.[11] Depths of fluorination reported ranged from 50 Å to 600 Å.[1-12] Decomposition mechanisms and the products of various gases used for plasma fluorination of polymer surfaces have been determined; however, the mechanism by which fluorination of hydrocarbon polymers occurs has not been completely established.[13-17] Fluorination of the polymer surface is achieved at carbon

sites by exposure of the polymer surface to reactive fluorine species in a plasma.

Several investigations of plasma fluorination of hydrocarbon polymers have also reported increases in atomic oxygen at the substrate surface after plasma fluorination.[5,8] Three mechanisms proposed to explain the surface oxidation include; 1) reaction of the polymer surface with trace amounts of oxygen contaminants in the gas feeds, 2) reaction with oxygen contaminants within the plasma chamber, and/or 3) post-reaction of long-lived, plasma generated free radicals upon exposure to the atmosphere.[5,8] Free radical reactions are common in plasma processes and they may result in surface crosslinking, chain scissioning, and/or ablation. Chain scissioning may result in the formation of volatile products and subsequent fluorination of the newly formed chain ends thereby forming -CF_3 functionalities. As the result of the predominating free radical reactions, complete fluorination without oxidation has been difficult to achieve.

Variations in plasma parameters have been shown to affect the type of active species produced in the plasma, the depth of fluorination, and the type of fluorination which results. Plasma parameters which can be varied include: gas feed composition, gas inlet flow rate, pressure, power, substrate/plasma temperature, placement of the sample in the chamber relative to the glow region, and time of exposure. Many of the parameters are interdependent, i.e., a variation in one parameter will cause a variation in another.

For this thesis project a poly(ester sulfonic) acid anionomeric membrane was exposed to both $CF_4/O_2/Ar$ and CF_4/Ar plasmas under

various conditions to determine which conditions would produce a maximum in fluorination with minimal surface etching and/or degradation. The effects of power, temperature, placement of the sample in the plasma chamber, oxygen in the gas feed and time of exposure on the extent of surface modification produced were examined. Three types of surface modification of the poly(ester sulfonic) acid membrane of interest include: fluorination, etching, and degradation. Fluorination is the addition of atomic fluorine and/or fluorine containing functionalities to the chemical structure of the polymer through a chemical reaction. Etching is the process of removing atoms or molecules from the polymer surface by chemical reactions with gas phase particles to form volatile products. As a result of the etching process, material is removed from the surface leaving behind a surface chemically similar to the original surface. Degradation of the polymer surface also occurs as the result of chemical reactions, but leaves behind a chemically and physically different surface.

The AQ55 membrane is used as an ion exchange membrane coated on the surface of an electrochemical detector for applications in flow injection analysis (FIA) and high performance liquid chromatography (HPLC). The ultimate goal of this project was to increase the chemical stability of the AQ55 membrane under aqueous flow conditions as well as increase the partitioning of large hydrophobic ions into the membrane by generating a hydrophobic surface. This project was designed to determine which plasma parameters would maximize surface fluorination while minimizing surface degradation and etching of the AQ55 surface.

In the following section the theory behind the use of a fluorocarbon plasma for surface fluorination of hydrocarbon polymers is discussed. Also included are: how a plasma is generated, types of species produced in a fluorocarbon plasma, control of the plasma parameters, and how each of these factors affects the resulting surface modification of the polymeric material.

1.1. Theory

A plasma is a partially ionized gas which contains an equal number of positive and negative ions/charges and a different number of neutral species. Typically there is a ratio of one charged particle to every 10,000 neutral particles. A block diagram of a plasma chamber is shown in Figure 1. A

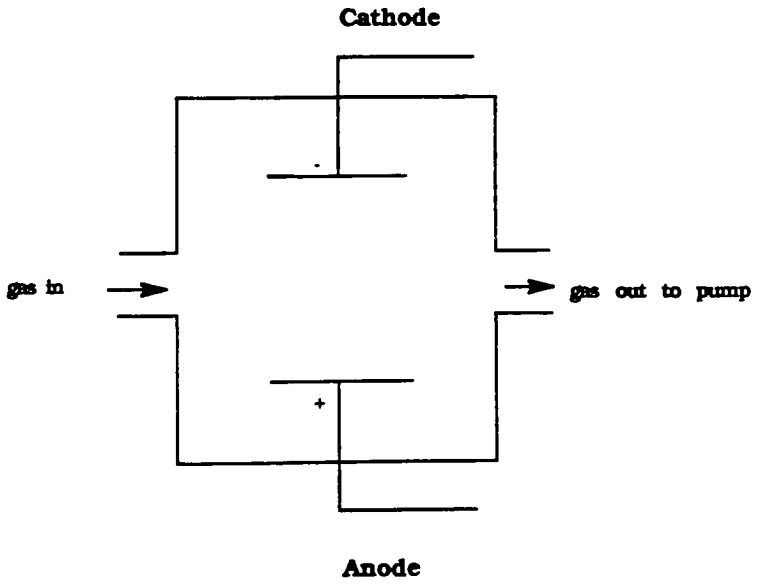

Figure 1: A block diagram of a plasma reactor chamber.

plasma is generated by applying an electric field to a gas or gas mixture at pressures typically between 0.1 and 1 torr. First a gas or gas mixture is bled into the evacuated chamber which contains the electrodes. Initially the gas contains a small amount of electrons as a result of the absorption of gamma radiation and/or natural radioactivity. When power is applied to the electrodes, electrons present in the gas begin to accelerate toward the anode, simultaneously, the positive charges are accelerated towards the cathode. Electrons absorb the same energy from the electric field as the ions, but retain more of it in inelastic collisions with neutral gas molecules. Acceleration of the charged particles causes an increase in gas phase collisions to occur. As a result, more charged and chemically reactive species are produced.

The different gas phase collisional processes which occur within a plasma include: ionizations, excitations, relaxations, recombinations, dissociations, and attachments.[18,19] Collisions occur between all possible permutations of ions, neutrals, and electrons.

Ionizations and excitations occur as a result of collisions, or by the absorption of energy from a photon or heat. An ionization occurs when a weakly bound electron is ejected from a neutral atom. In an excitation process an electron absorbs only enough energy to be promoted to a higher energy level in the same atom. In most excited states the atom or molecule is very unstable, therefore the electron will return to the ground state rather quickly by emitting a photon in the visible region. Plasmas are commonly called glow discharges because of this fluorescence phenomena. Recombinations occur when two oppositely charged species combine to form a neutral atom or molecule. Dissociation occurs when gas molecules are

fracture as the result of collisions with ions, electrons or neutral gas species. Finally, attachment occurs when an atom or molecule is reduced by an inelastic collision with an electron forming a negative ion.

As a result of these collisional processes, chemically active species can be produced within a plasma that are useful for material modifications. The material can be placed within the plasma stream allowing the surface atoms on the material to react with the active gas species, thereby chemically modifying the surface.

In designing a plasma experiment there are many parameters that can alter the physical and chemical properties of the plasma. These parameters include; gas feed composition, gas flow rate, chamber pressure, substrate/plasma temperature, power, time of exposure and placement of the sample in the chamber. The means by which each of the above parameters are controlled and how they can be varied to design an experiment for surface fluorination will be discussed in more detail in the following text.

1.1.1. Gas Feed Composition

The gas feed composition is considered the most important parameter because it determines the type of active species produced within the plasma, and therefore the type of plasma-surface interactions produced. The gas feed composition should contain a gas or gas mixture which produces the type of modification desired at the surface. Common gas choices for surface fluorination include: F_2/He,[1] F_2/Ar,[3] SF_6,[7,8] SF_6/He,[5] CF_3H,[4,6] CF_3Cl,[4,6], CF_3Br,[4,6] C_2F_6,[7,8] CF_4,[4,6-8,11] CF_4/He,[5] CF_4/Ar,[5] CF_4/O_2,[10,11] and $CF_4/O_2/Ar$.[9,12] Fluorocarbon gas feeds have been widely used together with

oxygen to promote surface etching. This is of specific interest in microelectronic technologies for the development of photoresist patterns and etching of silicon surfaces.

Decomposition mechanisms for CF_4 and CF_4/O_2 plasmas have been determined through the use of optical emission and mass spectrometry.[13] Emission spectroscopy with actinometry and mass spectrometry are both effective tools for *in situ* determinations of the type and relative amounts of stable and unstable reactive species produced in a plasma. In optical emission spectroscopy, a low concentration of an inert gas, typically argon, helium, or nitrogen is allowed into the gas feed to serve as a reference. The emissions of the other species are measured relative to the inert gas. The reactive species are mass analyzed by extracting the neutral species from the plasma tube via a gas sampling system. The neutral species are ionized with 20 eV electrons, and the positive ions produced are mass analyzed.

Decomposition of CF_4 is characterized by high concentrations of atomic fluorine and lower concentrations of CF and CF_2 radicals. Species detected in the effluent by mass spectrometry include CF_3^+, $C_2F_4^+$, and $C_2F_5^+$. These fragments suggest CF_2 and CF_3 radicals are formed in the plasma.[13] From these results the decomposition mechanism shown in Figure 2a was postulated. The primary decomposition is the result of an electron impact initiated reaction. Subsequent decomposition pathways occur through the mechanisms depicted in Figure 2b.

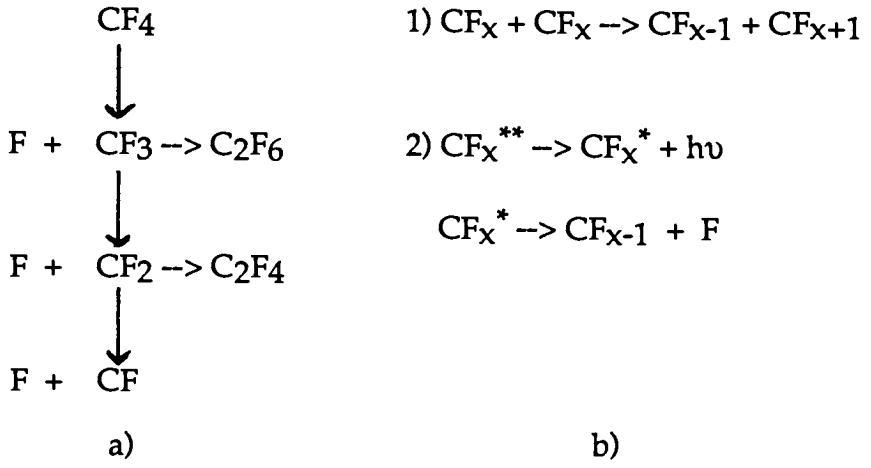

Figure 2: a)The proposed decomposition mechanism for CF_4. b) Mechanisms for subsequent dissociations after initial electron impact.[13,15]

The products detected by mass spectrometry were assumed to be formed from atomic fluorine, •F, •CF_3, and •CF_2 radicals.[13] All of the dissociation products shown in Figure 2 can potentially react with the polymer surface. Thus, it is possible that •CF_3, •CF_2, and •CF functionalities may graft to the polymer surface through radical reactions. Atomic fluorine is high in concentration and may also react with the polymer surface.

The concentration of CF and CF_2 radicals was drastically reduced as a result of the addition of oxygen to the gas feed.[13] Figure 3 shows the plots of relative intensity of CF and CF_2 as a function of percent oxygen in the gas feed. The concentration of CF_2 underwent a greater reduction than the CF as a result of the addition of O_2 to the gas feed. Therefore, in the presence of oxygen, fluorination would be expected to be dominated by reactions of the surface matrix with atomic fluorine and not by the grafting of CF_x functionalities to the polymer surface.

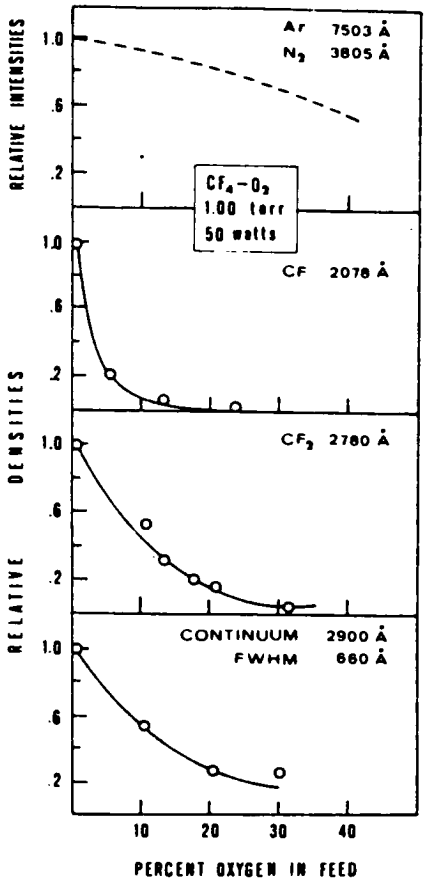

Figure 3: Plots of the relative intensity of CF and CF_2 present as a function of percent oxygen in the gas feed. [13]

Small additions of CF_4 gas to oxygen gas feeds has been found to increase the atomic oxygen concentrations in the plasma relative to a pure oxygen gas feed. An increase in the atomic fluorine concentration is also observed with small additions of oxygen to CF_4 gas feeds.[17] This is either a

result of the reaction between electronically excited metastable oxygen and CF_4 or between oxygen and dissociation products of CF_4.

Reaction products downstream of a CF_4/O_2 plasma are listed in Table 1.[17] Five of the reactions are electron induced dissociations and the remaining eight are free radical reactions.

Table 1: Reaction products downstream of a CF_4 / O_2 plasma. The rates of the reaction given were determined at a pressure of 0.5 torr.[17]

Reaction number	Reaction	Rate coefficient at 0.5 torr[a]	Notes
1	$CF_4 \xrightarrow{e} CF_3 + F$	6	b,c
2	$CF_4 \xrightarrow{e} CF_2 + 2F$	14	b,c
3	$CF_3 + F \xrightarrow{M} CF_4$	1.3×10^{-11}	e
4	$CF_2 + F \xrightarrow{M} CF_3$	4.2×10^{-13}	e
5	$O_2 \xrightarrow{e} O + O$	20	b
6	$CF_3 + O \rightarrow COF_2 + F$	3.1×10^{-11}	
7	$CF_2 + O \rightarrow COF + F$	1.4×10^{-11}	
8	$CF_2 + O \rightarrow CO + 2F$	4×10^{-12}	
9	$COF + O \rightarrow CO_2 + F$	9.3×10^{-11}	
10	$COF + F \xrightarrow{M} COF_2$	8×10^{-13}	e
11	$COF_2 \xrightarrow{e} COF + F$	20	b,d
12	$CO_2 \xrightarrow{e} CO + O$	40	b
13	$F + CO \xrightarrow{M} COF$	1.3×10^{-15}	e

[a] Units of s^{-1} (for first-order reaction) or $cm^3 s^{-1}$ (for second-order reaction).
[b] Rate quoted is for discharge region; reduced to a negligible value downstream from the plasma.
[c] The overall rate of reactions (1 + 2) is based on the measured % conversion of CF_4 at long residence time and large dilution by O_2 by Smolinsky and Flamm
[d] Set equal to $(k_1 + k_2)$.
[e] Reaction in fall-off region.

From the interpretation of Table 1, plasmas which are rich in CF_4 rapidly produce CF_2 at a rate about twice that of the production rate for CF_3. Plasmas rich in O_2 consume CF_x fragments by reaction with atomic oxygen and inhibit CF_4 reassociation. Free radical reactions with atomic oxygen play

an important role in the production of atomic fluorine as noted by reactions 6 through 9. Therefore, the addition of oxygen to CF_4 gas feeds will result in fluorination dominated by reactions with atomic fluorine. Atomic oxygen is produced primarily by an electron induced dissociation (reaction 5). Therefore increases in atomic oxygen formation can be correlated with the increases in electron densities observed with larger additions of CF_4 to oxygen plasmas.[17]

Figure 4 shows the relative optical emission intensities of atomic oxygen and atomic fluorine as a function of the percent CF_4 in O_2 gas feeds.[17]

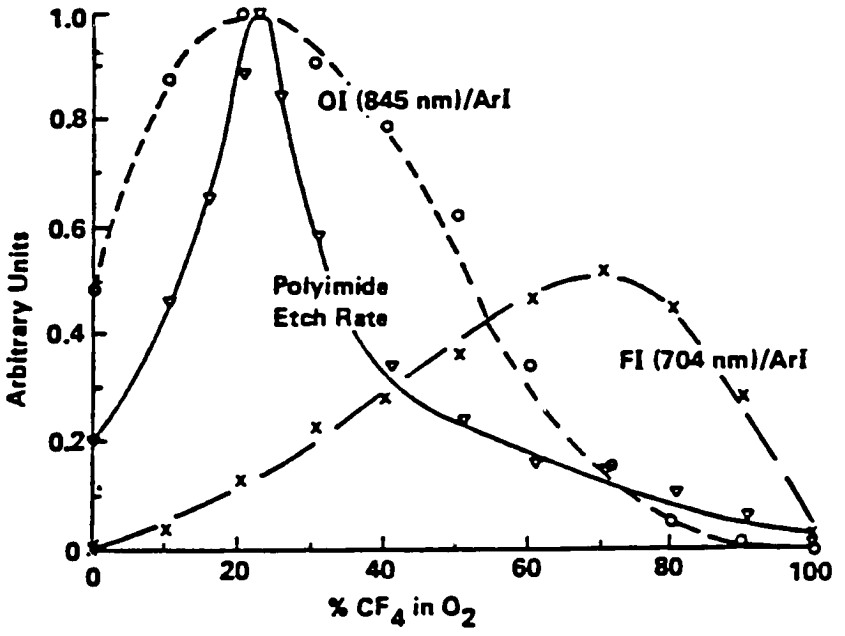

Figure 4: Relative emission spectral line intensities for atomic oxygen and fluorine at 845 and 704nm, respectively, using mixtures of oxygen and CF_4. Intensities are corrected using ArI 750.4nm. Also shown is the etch rate of polyimide, normalized to relative atomic oxygen concentrations.[17]

The production of atomic fluorine is maximized at approximately 60% to 80% CF_4 in O_2, while the production of atomic oxygen is maximized at approximately 20% CF_4 in O_2. Also shown in figure 4 is the etch rate of polyimide as a function of the percent CF_4 in O_2. The etch rate maximum is normalized with the maximum in atomic oxygen emission intensity and occurs at approximately the same composition. This indicates that the production of atomic oxygen, and therefore the presence of CF_4, plays an important role in the etching mechanism.

Proposed mechanisms for fluorination and etching of both saturated and unsaturated hydrocarbon polymers are shown in Figure 5.[17] The addition of atomic fluorine is the initiating step in both etching and fluorination reactions. Atomic fluorine within the plasma can react with the saturated polymer surface via a hydrogen abstraction mechanism.

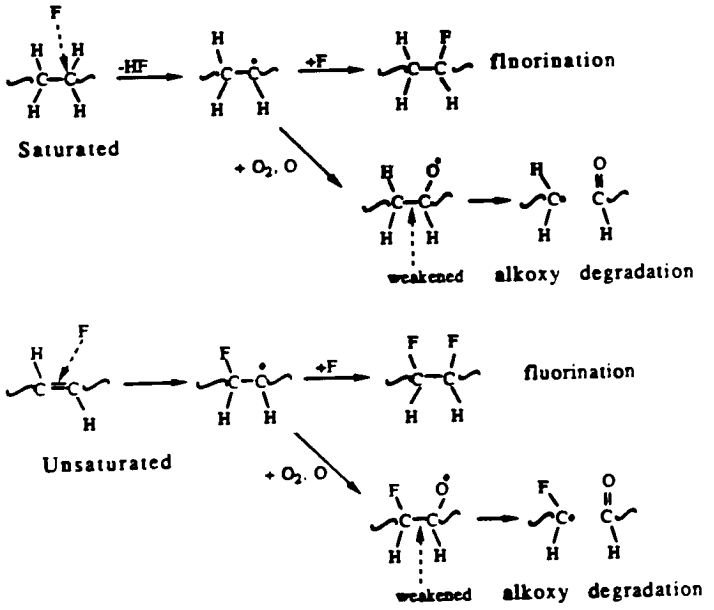

Figure 5: Possible reaction pathways of saturated and unsaturated hydrocarbon polymers in the presence of atomic oxygen and fluorine.[17]

The resulting free radical can either react with oxygen (molecular or atomic) or atomic fluorine. Addition of oxygen to the radical site weakens the adjacent carbon-carbon bond by forming an unstable alkoxy radical intermediate, which then cleaves through an alkoxy degradation mechanism. Unsaturated polymers first react with atomic fluorine by breaking the carbon double bond, adding a fluorine and thereby producing a radical on the adjacent carbon. This radical proceeds through the same mechanisms for fluorination and etching as shown for the saturated polymer. In both the saturated and unsaturated case there is a significant competition between degradation/etching, which results from oxygen adding to the radical site, and fluorination which results from fluorine adding to the radical site. Therefore, high concentrations of CF_4 and low concentrations of oxygen would be favorable for surface fluorination of hydrocarbon polymers. Low concentrations of CF_4 in an oxygen plasma would be favorable for surface etching. Elimination of oxygen from the gas feed would decrease the occurrence of alkoxy degradation. However, small additions of oxygen to CF_4 gas feeds have been shown to increase atomic fluorine concentrations in the plasma relative to fluorine concentrations found in the pure CF_4 plasma. Therefore small additions of oxygen to CF_4 would be expected to increase the degree of fluorination relative to a pure CF_4 plasma, however, this has not been determined yet.

The affinity of the polymer for atomic fluorine changes with the degree of unsaturation within its chemical structure. Unsaturated polymers have greater affinities for atomic fluorine that their saturated counterparts. As a result the saturated polymers will require larger concentrations of atomic

fluorine, i.e., small additions of oxygen in a CF_4 plasma, to begin either the fluorination or the etching mechanism.

Investigations on plasma etching and fluorination of structurally different polymers with different percentages of CF_4 in O_2 have been reported.[17] Plots of the etch rates versus the percent CF_4 in O_2 for polyimide, polyisoprene, and polyethylene, as well as each of the polymer chemical structures are found in Figure 6.[17] A maximum in etch rate is seen for all three polymers in the oxygen rich region, which can be correlated with an increase in the formation of atomic oxygen at these compositions. However, the gas composition at which these polymers reach their maximum etch rate is proportional to the degree of unsaturation in the polymer structure.

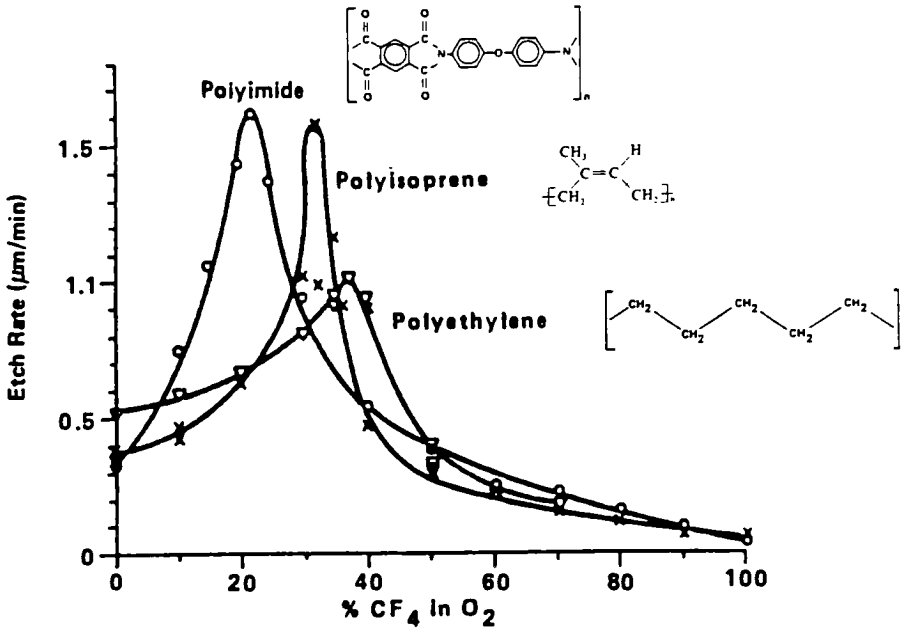

Figure 6: Etch rates of polyimide, polyisoprene, and polyethylene downstream of CF_4/O_2 plasmas.[17] Also shown are the structures of each polymer.

Therefore the affinities of these polymers for atomic fluorine follows polyimide > polyisoprene > polyethylene. As the polymer's affinity for atomic fluorine decreases, the concentration of CF_4 required to reach a maximum etch rate increases. Rapid decreases in etching rates are observed above approximately 50% CF_4 where the atomic fluorine begins to compete with the atomic oxygen for the radical site on the polymer backbone and fluorination begins to predominate.

Fluorine enhances degradation by the formation of the radical site. However, excess fluorine competes with oxygen for the radical sites thereby inhibiting the formation of volatile etch products. Therefore higher levels of fluorine with concurrent decreases in oxygen concentrations increases polymer surface fluorination. For most polymers, maximum fluorination is observed above CF_4 concentrations of about 80% in oxygen gas feeds.

1.1.2. Flow Rate

The gas flow rate is controlled by the volume of gas allowed into the chamber per unit time as well as the evacuation rate. Gas flow rates are measured in standard cubic centimeters per minute (sccm). Two terms which describe the flow rate include the pumping speed (S) and the throughput (Q).[19] The pumping speed is the volume of gas moving through the system per unit time. The number of molecules contained in that volume is directly proportional to the pressure of the gas and is related to the throughput. The throughput (Q) is calculated by:

$$Q = p \times S \tag{1}$$

where p is the pressure of the gas. The throughput is more commonly called flow rate, and is proportional to the flux of gas molecules through the chamber. As the number of molecules in the chamber increases (by increasing the inlet gas flow), the pressure and throughput increase.

The residence time (τ) is defined as the average time the gas spends in the chamber before it is evacuated. The value of τ can be calculated by;

$$\tau = \frac{p \times V}{Q} = \frac{V}{S} \qquad (2)$$

where V is the total volume of gas. For both etching and fluorination reactions, as the active species are consumed by the substrate, the inlet flow rates must be increased to replenish the active species within the plasma. The pumping speeds must also be increased to remove any by-products from the plasma-surface reactions which may contaminate the surface of the substrate by further reaction. As a result, low residence times and high throughputs increase the supply rate of fresh active species to the material surface, which is favorable for both fluorination and etching. Plasmas rich in CF_4 at high throughputs will increase the rate at which atomic fluorine is supplied to the surface and thereby increase fluorination. Plasmas rich in oxygen at high throughputs will increase the rate at which atomic oxygen is supplied to the surface and thereby enhance the etch rate.

Fluorination of polyethylene surfaces with a F_2/He plasma was shown to be enhanced with increases in gas flow rates.[2] The effect of flow rate on the percent atomic fluorine at the polyethylene surface is shown in Figure 7. Results at two pressures and two treatment times are shown. Rapid increases

in percent atomic fluorine are observed between 20 sccm and 30 sccm. Increases in pressure and treatment time are also shown to increase the rate at which percent atomic fluorine is maximized. Beyond a flow rate of 40 sccm the percent atomic fluorine remains relatively constant. Therefore, in this case, a minimum of 40 sccm would be necessary to achieve rapid fluorination at small reaction times.

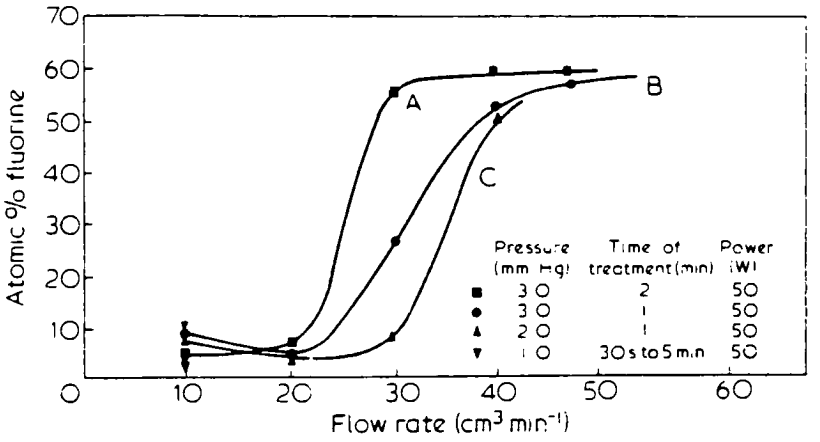

Figure 7: Atomic percent fluorine detected at the surface of polyethylene as a function of flow rate. Atomic percent fluorine determined by XPS.[2]

1.1.3. Pressure

The pressure is controlled both by the amount of gas allowed into the chamber per unit time and the evacuation rate. By increasing the inlet flow rate while keeping the evacuation rate constant, the number of gas phase particles in the chamber increases, the number of gas phase collisions increases, and therefore the pressure increases. At constant inlet flow rates, higher evacuation rates will decrease the number of gaseous particles in the chamber, and pressures will decrease.

Variations in pressure can affect the rate of plasma-surface reactions and the energy with which the reactive gas phase species strike the surface of the material. Referring to Figure 7, an increase in pressure from 2 mmHg to 3 mmHg (at constant power) was shown to increase the atomic percent fluorine detected at the surface of polyethylene after exposure to a F_2/He plasma. This was expected since an increase in pressure is proportional to an increase in the concentration of active species in the plasma, which in this case caused fluorination.

The energy of the plasma is proportional to the ratio of power applied on the electrode to the pressure of the gas. At constant power increases in pressure will decrease the plasma energy. Since more gaseous species are present at high pressures gas phase collisions are increased. Gas particles lose energy with each collision, therefore they will strike the substrate with a lower energy at higher pressures. At low pressures, there is a smaller number of species present, and the number of collisions decrease. With fewer gas phase collisions, the gaseous species will strike the surface with more energy and can thereby modify or damage the polymer surface. Ion bombardment of

the substrate surface is believed to generate free radical sites on the polymer surface.[23]

For surface fluorination, the advantages of working at high pressures is twofold. High pressures increase the concentration of reactive species near the surface of the substrate and eliminate surface damage by collisions with high energy gaseous particles. At constant evacuation rates, high pressures are obtained by using high flow rates.

1.1.4. Power

The energy of the plasma is proportional to the ratio of the applied power to pressure. At constant pressure, an increase in power results in an increase in plasma energy. Variations in power have more of a direct effect on the formation of active species in the plasma than on the substrate. High power inputs will increase the acceleration of gas phase particles and thereby increase the production of active species through collisional processes. This enhances the supply of reactive species to the substrate and increases the probability of a plasma-surface reaction. In a CF_4 rich plasma, an increase in input power should enhance fluorination by increasing the supply rate of atomic fluorine and CF_x species. In an oxygen rich plasma increases in atomic oxygen production and etch rates would be expected to occur with increases in power.

The effect of radio frequency (RF) power variations on the extent of fluorination of polyethylene with F_2/He plasmas has been reported.[2] Plots of percent atomic fluorine detected at the surface of polyethylene films after exposure to 25 W, 50 W and 100 W plasma are shown in Figure 8. No

significant changes in the extent of fluorination were observed as power was varied, which is contrary to the expected behavior. In another study, an exponential increase in etching rates of polyimide were found with increases in power.[22] This increase in etch rate with power correlated with the temperature increases observed with increasing power. Therefore, the applied power appears to indirectly affect etching rates and not fluorination.

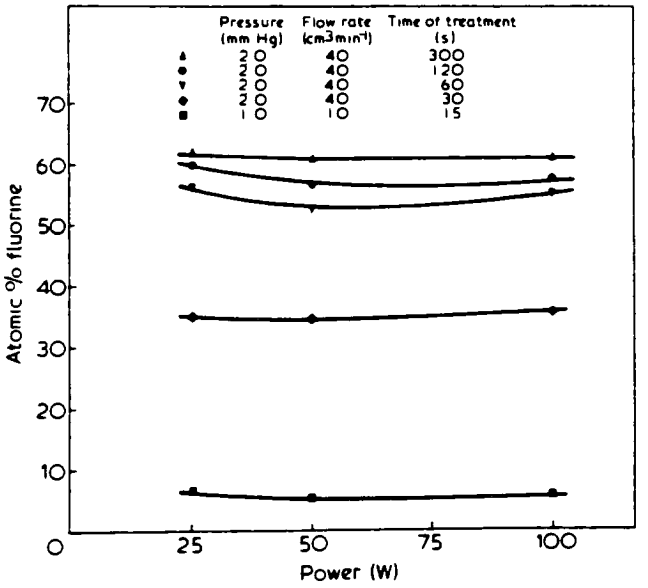

Figure 8: The effect of RF power variations on the extent of fluorination of polyethylene with F_2/He plasmas.[2]

1.1.5. Substrate/ Plasma Temperature

In general the rates of reactions are related to temperature by the Arrhenius equation: [17,19]

$$k' = A \exp[-E_a / kNT] \quad (3)$$

where k' is the rate constant, A is the frequency factor, E_a is the activation energy, k is the Boltzmann constant, N is Avogadro's number, and T is the temperature. The activation energy for plasma-surface reactions is actually a summation of the activation energies for a series of reactions including: the formation of reactive gaseous species, diffusion of the active species to the polymer surface, adsorption by the surface, reaction with the surface, desorption, and diffusion of reaction by-products away from the polymer surface. Generally, rate constants are directly proportional to temperature. As a result, an increase in fluorination rates is expected as the temperature is raised for CF_4 rich plasmas. Higher etch rates are likely with increases in temperature for oxygen rich plasmas. When working with polymeric materials, as the temperature of the material nears the Tg, the polymer gains molecular mobility and the probability of depropagation is higher. Excessive depropagation of the polymer chains results in the removal of material from the surface of the polymer in the form of low molecular weight fragments. Therefore, etching and/or surface degradation rates are accelerated as the glass transition temperature of the polymer is approached regardless of what gas composition is used.[21] In a fluorine rich plasma the competition between etching and fluorination will be more apparent at higher temperatures.

Eventually etching will predominate leaving behind a surface which is only partially fluorinated. As a result of this temperature sensitivity, precautions must be taken to ensure that the substrate remains below its glass transition temperature during plasma exposure if etching and/or degradation are not desired.

The effect of substrate temperature on etching of poly(methylmethacrylate) (PMMA) surfaces has been studied.[21] Arrhenius plots of the temperature dependence of PMMA etching rates during exposure to CF_4 rich plasmas are shown in Figure 9. Etching rates rapidly accelerate above 60-90°C as a result of both depropagation reactions and chain scissioning reactions. The chain scissioning reactions are shown to vary with oxygen concentrations in the gas feed.[21]

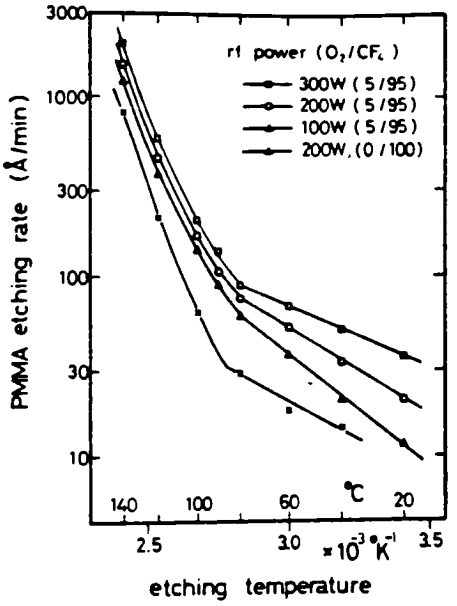

Figure 9: Etching rates of PMMA as a function of temperature.[21]

The affinity of the polymer for the reactive species within the plasma changes with temperature. In Figure 10 the etching rate of polyimide as a function of percent CF_4 in O_2 is plotted for two different temperatures.[7] As the temperature is increased to 70°C, the maximum etching rate increases. This suggests that the activation energies of reactions producing volatile etch products are being overcome by increases in temperature. Depropagation would be expected to aid in the increased etch rate, however since the Tg of polyimide is exceptionally high, any depropagation produced was not a result of the temperature exceeding the Tg. The maximum etch rate was achieved at a higher percent of CF_4 in oxygen at higher temperatures, indicating an increased affinity for atomic oxygen with temperature. As a result, when working at high CF_4 concentrations and elevated temperatures, the substrate will have an increased affinity oxygen. Therefore, increases in etch rates may still be observed at higher temperatures in CF_4 rich plasmas.

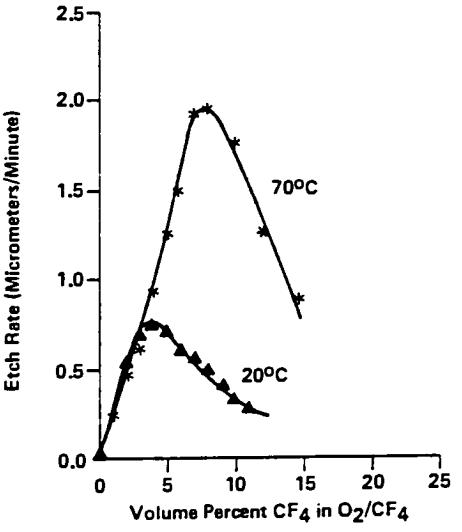

Figure 10: Etch rate of polyimide downstream from a CF_4/O_2. microwave plasma at two different temperatures.[17]

1.1.6. Time of Exposure

The degree of surface modification that takes place is proportional to the time frame of the experiment. If the time of exposure is shorter than the kinetic time frame of the fluorination and/or etching reactions, minimal amounts of modification will take place. Typical times of exposure examined have been in the range of 30 seconds to 60 minutes.[1-12] Within this range of time, the competition between fluorination and etching (and/or degradation) is significant. Fluorination of the polymer surface may occur, yet as the number of free radical reactions increases, the number of fractured chains and volatile fragments will increase. As a result, the initially fluorinated polymer chains may be removed leaving behind a new surface which can be modified further with time. This cycle of fluorination and etching can continue resulting in small depth of modification because of the removal of previous surface layers.

The degree of modification is also affected by changes in temperature. As previously mentioned, increases in temperature result in direct increases in reaction rates. Therefore, the effect exposure times have on plasma modification is controlled by kinetic as well as thermodynamic factors. At constant exposure time, increased temperatures will result in the acceleration of reaction rates and a higher degree of surface modification. A similar effect is achieved with increased exposure times at constant temperatures.

The atomic concentrations found on the surface of polyimide after exposure to a 85% CF_4 / 10% O_2 / 5% Ar plasma at various exposure times are shown in Figure 11.[10] The percent atomic fluorine found on the surface increases with exposure time until a steady state is achieved at approximately

30 minutes. Figure 12 is an illustration of a Rutherford Backscattering Spectroscopy (RBS) spectrum for a sample fluorinated for 5 minutes.[10] Depths of fluorination can be estimated by the width of the fluorine signal. The calculated depths of fluorination are depicted as a function of exposure time in the insert plot of Figure 12.[10] A linear relationship between depth of fluorination and time exists between 1.5 minutes and 10 minutes. Fluorination rates decrease at longer exposure times. This fluorination profile suggests that fluorination is diffusion controlled. Similar results were found for low density polyethylene fluorinated with a CF_4/O_2 plasma.[22]

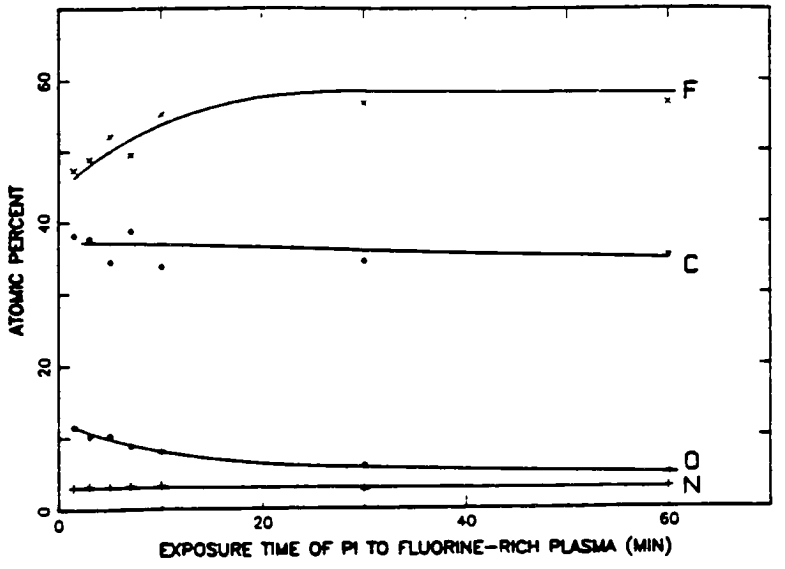

Figure 11: The atomic concentrations found on the surface of polyimide after exposure to various fluorination times. Atomic concentrations determined by XPS .[10]

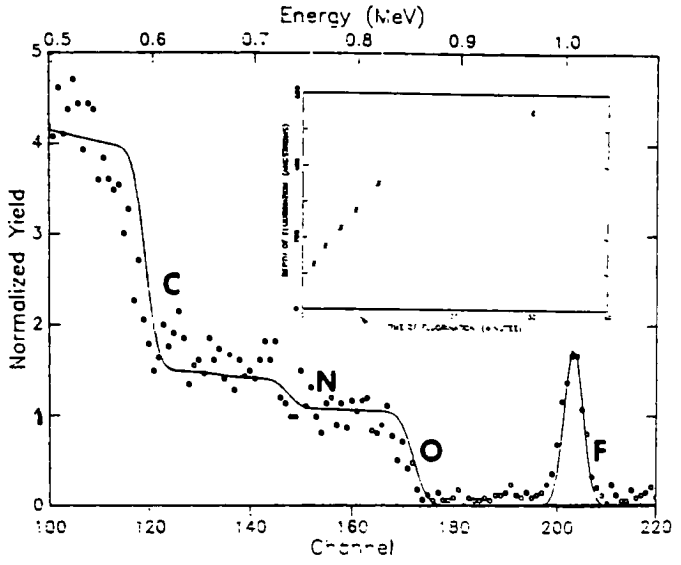

Figure 12: Experimental and calculated RBS spectra for polyimide after a 5 minute exposure time. The insert plot shows the calculated depth of fluorination as a function of exposure time.[10]

1.1.7. Placement of the Sample in the Chamber

The type of surface modification produced by a plasma can be significantly affected by the position of the sample in the chamber relative to the glow discharge region. Generally, the further the sample is placed from the glow, the "softer" the modification becomes. This does not imply that less modification occurs; rather, the amount of high energy ion bombardment decreases as the distance of the sample from the glow is increased. Ion bombardment increases the formation of surface radical sites which may promote surface etching and/or degradation.[22]

Shielding the polymer sample with a quartz disc is one technique which changes the placement of the sample within the glow.[20] Egitto et.al.

placed the polyimide sample on the cathode surface with a quartz disk 0.32 cm above the sample (Figure 13a).

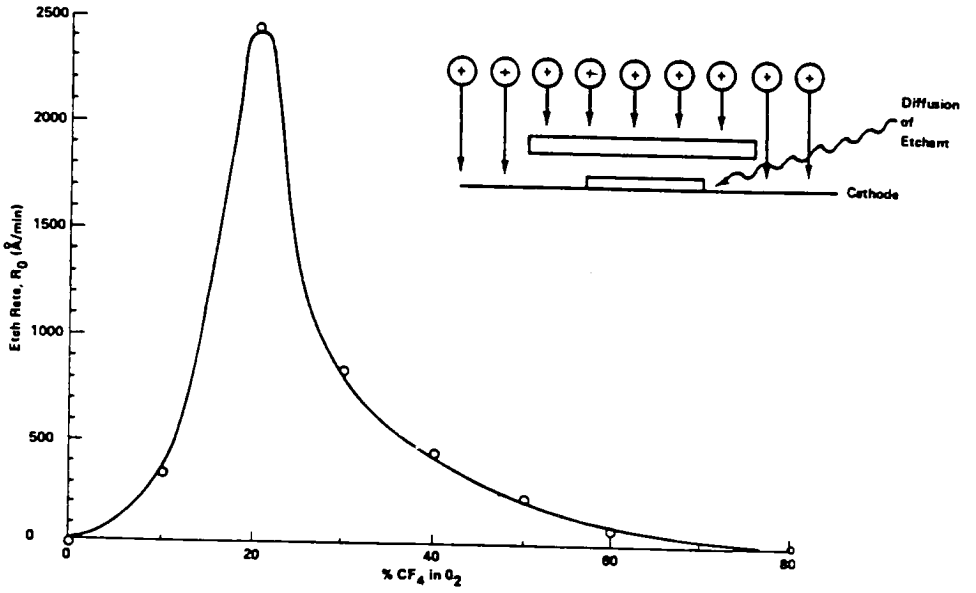

a) With the quartz plate shield.

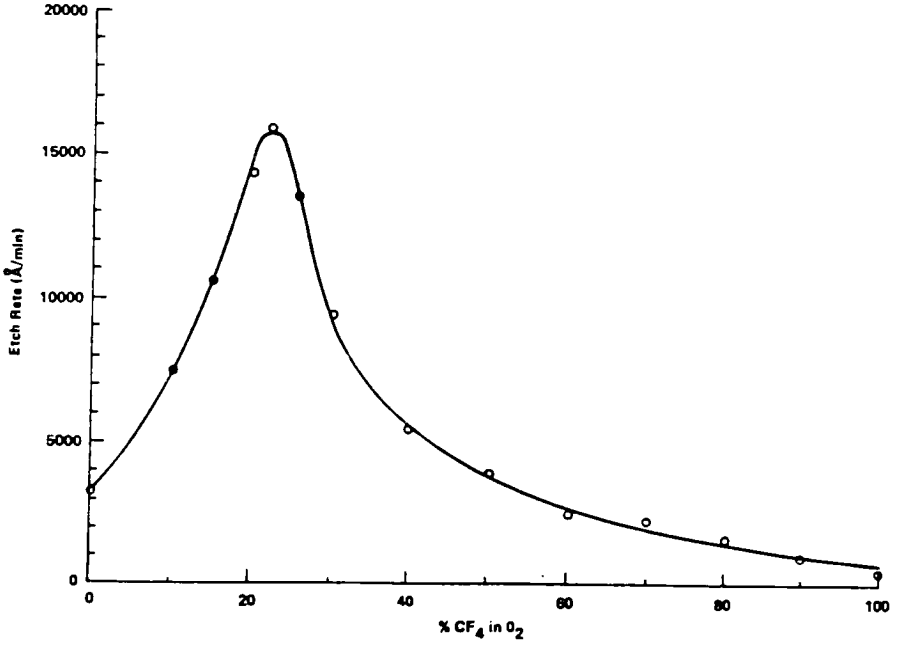

b) Without the quartz plate shield.

Figure 13: Polyimide etch rates a) with and b) without the quartz plate shield as a function of %CF_4 in O_2 .[20]

This removed the polymer sample from the most energetic part of the glow discharge and eliminated bombardment of ions on the polyimide surface. Diffusion of reactive species to the polymer surface below the quartz plate was still possible. Shielding of the substrate with the quartz plate decreased the etching rates significantly in the oxygen rich plasmas, Figure 13.[20] A maximum etching rate of ~16000 Å/min was achieved without the quartz plate (Figure 14b), while a maximum of only ~2500 Å/min was achieved with the quartz plate shield. It should also be noted that etching rates dropped to zero above 80% CF_4 in oxygen with the quartz plate shield.

1.2. Thesis Project Design

The polymer of interest for this thesis work was a poly(ester sulfonic) acid anionomeric membrane, more commonly called AQ55 (Figure 14). The name AQ indicates that the polymer is water dispersible and the 55 signifies the ionomer's glass transition temperature of 55°C. AQ55 is classified as an ionomer which is defined as a copolymer containing up to 15 mole percent of ionic pendent groups per repeat unit. The presence of these ionic pendent groups can produce dramatic changes in the physical and chemical properties of the polymer, which has led to a rise in the number of applications for ionomers over the past twenty years. The applications include; ion exchange membranes, biosensors, adhesives, membranes for municipal waste water treatment, etc.

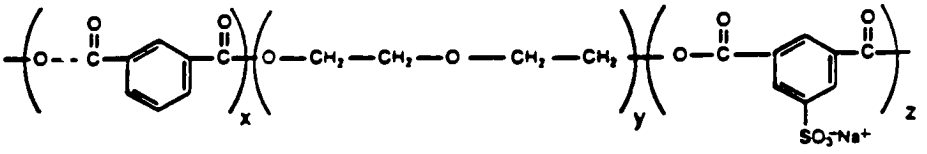

Figure 14: The structure of the poly(ester sulfonic) acid, AQ55.

The ultimate objective of this work was to surface fluorinate the AQ55 membrane to increase its chemical stability under aqueous flow conditions, as well as to increase the partitioning of large hydrophobic ions into the membrane by generating a hydrophobic surface. The partitioning coefficient

is defined as the ratio of the concentration of analyte exchanged into the membrane to the original concentration of analyte in solution. The immediate goal was to determine which plasma parameters would produce the maximum fluorination with minimal surface etching and/or degradation. The different plasma parameters which were varied include: gas composition, power, time of exposure, and the placement of the sample in the chamber.

Gas compositions examined included an 85% CF_4 / 10% Ar / 5% O_2 mixture and a 90% CF_4 / 10% Ar mixture. CF_4 rich plasmas were examined since they have been shown to produce high degrees of fluorination.[4-12] A plasma containing 5% oxygen was used to determine if the small addition of oxygen aided in fluorination by increasing the production of atomic fluorine or hindered fluorination by promoting surface etching/degradation through the alkoxy degradation mechanism.[17] An addition of 10% argon gas was made to all plasmas in order to increase the number of gas phase collisions which aid in the production of active species.

The radio frequency (RF) powers examined included 10 W, 20 W, and 50 W. Initial experiments indicated that 10 W was too low of power to sustain a plasma reproducibly, therefore the majority of the experiments were performed at 20 W or 50 W. In terms of the ratio of applied power to the cathode surface area the powers used included 0.399 W/cm^2, and 0.998 W/cm^2, which were similar to other experimental ranges examined in the literature.[1-22] Other experiments have shown that power affected etching rates, however, it was not a factor which affected the degree of fluorination. Therefore, two powers were examined to determine the affects of power on the type of modification produced.

Time of exposures were varied from 30 seconds to 30 minutes. At least three exposure times were examined for each set of conditions. It was expected that fluorination would increase with time of exposure and eventually reach a steady state when the competition between etching/degradation and fluorination was significant.

Two different placements of the samples in the chamber were examined. Samples were either placed on the cathode or they were placed on the cathode shielded by a quartz plate above the samples. The quartz plate was used to decrease ion bombardment and thereby limit or eliminate surface etching and/or degradation. This was expected to aid in fluorination by limiting the removal of fluorinated segments by ion bombardment and reactions similar to the alkoxy degradation mechanism described earlier.

Modified and unmodified AQ55 membranes were analyzed using XPS, FTMIR infrared spectroscopy, contact angle measurements, SEM, and gravimetric analysis to determine the type of chemical and physical modification made.

2.0. Experimental

2.1. Plasma System and Conditions

The plasma system used for surface fluorination is shown in Figure 15 and has been previously described.[24] The reactor contained a volume of 22700 in^3 with a cathode surface area of 8.29 in^2. The plasma was ignited by a 13.56 MHz radio-frequency (RF) generator (RF Plasma Products) inductively coupled to the reactor. An auto impedance matching network was coupled to the generator in order to minimize the reflected power to less than 1 W.

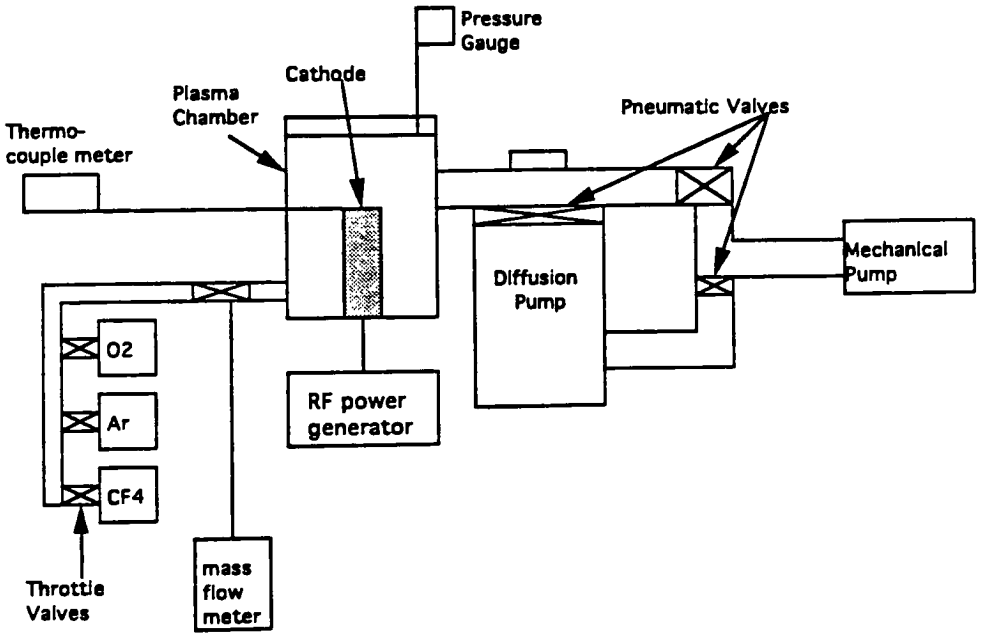

Figure 15: A diagram of the RF plasma system used for surface fluorination.

A more detailed diagram of the plasma chamber is shown in Figure 16. The cylindrical chamber was constructed from stainless steel with an inner diameter of 19 inches, 20 inches in height, with two cover plates of 19.5 inches diameter. The chamber was accessed by raising and lowering the top cover plate by a mechanical hoist. A 3 1/4 inch diameter cathode extended up from the base plate to a height of 14 inches. The cathode consisted of an aluminum cover plate surrounding a brass electrode. The electrode was connected to a copper conductor with a brass Swagelock fitting.

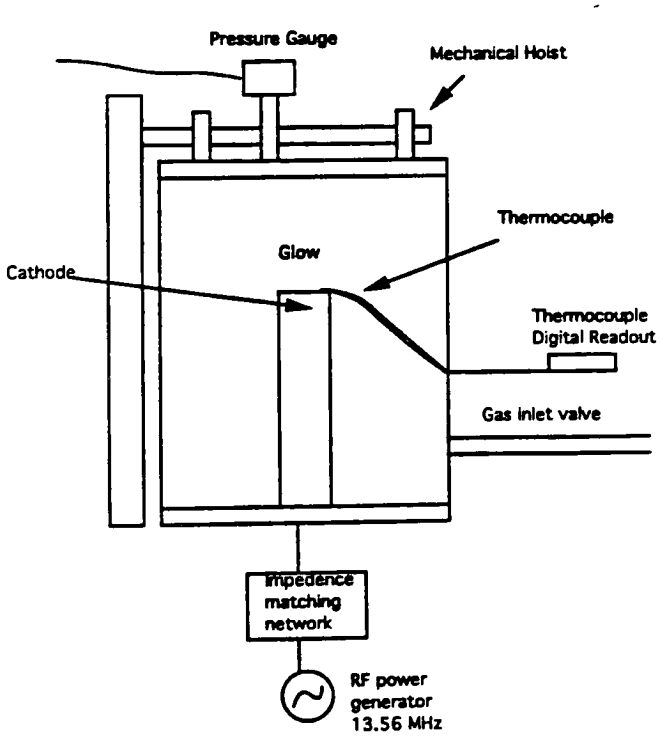

Figure 16: The plasma chamber.

Polymer samples were placed at the top surface of the electrode for modification, as shown in Figure 17. Samples were also modified with a quartz plate shield suspended 1.2 mm above the surface of the cathode to remove the samples from the glow discharge region. Glass spacers were used to support the quartz plate shield as shown in Figure 17.

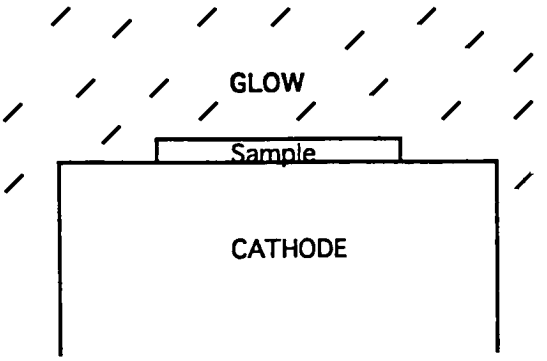

a) Without the quartz plate.

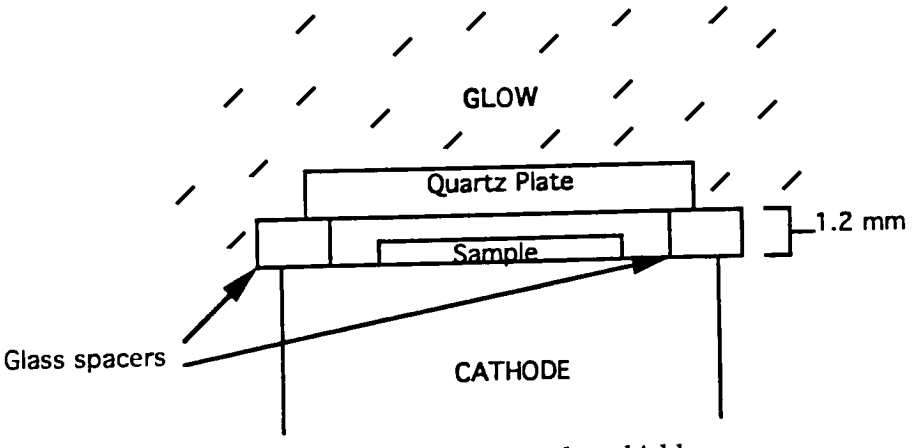

b) With the quartz plate shield.

Figure 17: Placement of the polymer samples at the a) cathode and b) at the cathode with a quartz plate suspended above the samples.

Once samples were placed into the reactor, the system was evacuated with a Welch Duo Seal mechanical pump (Model 1374) to approximately 60 mtorr. The chamber was backfilled with argon gas at approximately 40 standard cubic centimeters per minute (sccm) to +1 torr. Once the chamber pressure was held at +1 mtorr for 1 minute, the argon gas flow was turned off and the chamber was re-evacuated. This backfill procedure was performed three times to minimize atmospheric oxygen in the system. After backfilling, the chamber was evacuated to approximately 1-2 mtorr with a NRC Type 184, water cooled oil diffusion pump. Again the system was backfilled with argon gas three times. The chamber pressure was then stabilized at approximately 40 mtorr using only the mechanical pump. Finally, the system was backfilled once more with argon gas three times and then the chamber was evacuated to approximately 40 mtorr.

To establish the plasma gas composition, either a 10 : 90 (flow rate ratio) mixture of argon to CF_4 gas (2 sccm : 18 sccm) or a 5 : 10 : 85 (flow rate ratio) mixture of oxygen, argon, and CF_4 gas (1 sccm : 2 sccm : 17 sccm) was backfilled into the chamber at a total flow rate of 20 sccm. The argon and oxygen was purchased from Air Products and Chemicals Co. and the CF_4 gas was purchased from Matheson Inc. All three gases were used without further purification. The gases were turned on in order of increasing flow rate. All three gas regulators were set to a forward pressure of 20 PSI. A flow rate of 20 sccm was used throughout all experiments and was measured using a Hastings Mass Flow Meter, model ALL-50D. Once the pressure equilibrated, between 0.44 - 0.5 torr, the plasma was ignited at the given power until the desired exposure time had elapsed.

The plasma system was not equipped with a throttle valve between the chamber and vacuum system which limited control of the evacuation rates. As a result, pressures varied and are a direct function of the total gas flow rate, gas composition, and evacuation rates for a given experiment. Flow rates were kept constant, however, changes in gas composition altered the mass percent of gas entering the chamber. Additions of 5% oxygen to the gas flow increased pressures typically 50 mtorr. Evacuation rates were dependent upon the efficiency of the vacuum system at the time of the given experiment.

A thermocouple was used to measure the change in sample temperatures immediately after plasma exposure. A copper/constantan thermocouple was attached to a small piece of silicon wafer coated with the AQ55 dispersion. The piece of silicon was then adhered to the cathode next to the samples to be modified. Temperature measurements were read off an Omega digital readout, model DP116-TC1. Temperatures could not be read while the plasma was ignited because of interference from the RF power source. As a result, temperature readings were taken within 2 seconds after the RF power was turned off.

Variations in the gas composition, time of exposure, RF power and placement of the samples in the chamber were made to determine which parameters aid in maximizing fluorination and minimizing surface degradation.

2.2. Film Preparation

The poly(ester sulfonic) acid, AQ55, was purchased from Eastman Chemical Co. in a solid pellet form. Aqueous dispersions of 28% (wt/wt) AQ55 were prepared by stirring the pellets in ultra pure water (18MΩ) at approximately 80 °C overnight. Free standing films were solution cast on a Bytac® covered aluminum block in a 40 +/- 2 °C oven for at least 24 hours. Individual films were cut with a razor blade while the aluminum block was kept at 40 - 50 °C, thereby keeping the films soft enough to cut. Films were then pressed flat between two aluminum blocks covered with Bytac® on a Carver Laboratory Press, model M at 65 +/- 5 °C and 1200 lbs. pressure. Films were dried overnight in a VWR Scientific (Model 1410) vacuum oven at 70 +/- 2 °C and 30 inHg, and then stored in a vacuum desiccator. Both the vacuum oven and desiccator were evacuated with either a Welch DirecTorr V, Model 8920 vacuum pump or a Precision Scientific GCA, Model DD 195 vacuum pump, respectively.

Three inch diameter monitor silicon wafers obtained from Dr. Mike Jackson (Center for Microelectronic Engineering, RIT) were used as substrates for spin coated thin films. The wafers were cleaned with an oxygen plasma in the Tegal Plasmaline 415 plasma asher to remove any organic residue. This was followed by the RCA process (Appendix I) to obtain a native silicon surface. Clean wafers were allowed to stand in the ambient (25 +/- 5 °C and 1 atm) for at least 24 hours in order to grow a hydrophilic oxide layer which has a greater affinity for the AQ55 aqueous dispersion than the hydrophobic native silicon surface.

AQ55 films were spin coated onto silicon substrates in a class 1000 clean room at the Center for Microelectronic Engineering at RIT. The silicon wafers were heated to 70 +/- 2 ^{o}C for 5 to 10 minutes on a Digital Dataplate Hot Plate/Stirrer (Model PMC 730). Then approximately 10 ml of the AQ55 dispersion was dispensed through a 1 μm Gelman glass fiber acrodisc filter onto the silicon <111> or <100> surface while the wafers were held on a Headway Photoresist spinner (Model 1-EC101-R485). The dispersion was allowed to spread such that the entire surface area of the wafer was covered. The wafers were spun at 1000 to 2000 rpm for 2 minutes. Immediately following spin coating, the wafer was placed back on the hot plate for approximately 5 to 10 minutes to dry. The thin films were dried in vacuo overnight at 70 - 80 ^{o}C and then stored in a vacuum desiccator under a nitrogen atmosphere. Individual films were cut from the wafers using a diamond scribe.

2.3. Ion Exchange Chromatography

Ion exchange chromatography was used to purify the AQ55 dispersion into the Na^{+} form and exchange it into other sulfonate salt forms. A 150 ml fritted Pyrex ion exchange column was packed with approximately 75 ml of Amberlite IR-120 (plus) ion exchange resin (Aldrich, gel type, sulfonic acid functionality) in ultrapure (18MΩ) water. The ion exchange resin was washed with three resin bed volumes of ultrapure water, and then activated with three to four resin bed volumes of a 10% sodium hydroxide aqueous solution (Baker Analyzed, Reagent Grade). Approximately 20 - 30 ml of the 28% AQ55 dispersion was passed over the column and collected. The used

resin was rewashed approximately six times and repacked in ultrapure water. The same procedure was repeated two more times using fresh 10% sodium hydroxide solution and re-passing the same volume of AQ55 over the column. The AQ55 was collected at the end of three cycles over the column. This procedure was also followed to exchange AQ55 from the Na^+ form into the H^+ form using a 10% hydrogen chloride (Baker Analyzed, Reagent grade) activating solution.

2.4. Characterization of Unmodified and Modified Films

FTIR/MIR, contact angle measurements, X-ray Photoelectron Spectroscopy (XPS or ESCA), Scanning Electron Microscopy (SEM), and gravimetric analysis of the AQ55 film surfaces were performed before and after plasma exposure. The film bulk properties were analyzed by Differential Scanning Calorimetry (DSC).

2.4.1. Fourier Transform Infrared Spectroscopy (FTIR) with Multiple Internal Reflectance (MIR)

Fourier Transform Infrared Spectroscopy (FTIR) with the addition of a Multiple Internal Reflectance (MIR) apparatus provides information on the molecular functionalities at the surface of a material. Analysis of the AQ55 films was carried out on a Perkin Elmer FTIR, model 1760X, with a MIR attachment using a KRS 5 cell. All films were analyzed before and after plasma exposure from 4000 to 400 cm^{-1}, using 20 or 100 scans, 2 cm^{-1} resolution, a 45 degree incident beam angle, and an air background. Highly reflective aluminum foil (0.01mm thick) was used to cover the rubber

bumpers placed behind the samples to minimize any absorbence by the rubber and to maximize reflectance of the infrared beam. After the modified spectrum was taken, a difference spectrum was produced by subtracting the spectrum of the unmodified film from the spectrum of the modified film. Differences in film absorbtions before and after plasma exposure were then evident in the difference spectrum.

2.4.2. Contact Angle Analysis

Advancing, receding, and sessile drop contact angles were used to determine changes in surface energy caused by exposure of the AQ55 film to the plasma. A Rame-Hart Goniometer (Model 100 00 115) was used to make direct contact angle measurements. Both modified and unmodified surfaces were analyzed using a phosphate pH 7 Buffer (prepared from a stock solution of NaOH and Baker Analyzed reagent grade potassium phosphate) or Dimethyl Sulfoxide (Baker Analyzed Reagent Grade) as the contacting solvent.

2.4.3. X-ray Photoelectron Spectroscopy (XPS or ESCA)

The majority of the XPS analysis of the AQ55 surfaces was carried out at Xerox Corporation, Webster, New York by Dr. Thomas Debies using a Kratos Model XSAM 800 in both low and high resolution. Both quantitative elemental surface analysis as well as chemical structural information was obtained. The type of carbon functionalities produced at the surface can be determined from the shift in the binding energy of the C 1s peak. Film surfaces were analyzed without further modification or cleaning. The

analysis was carried out using Mg Kα radiation at 15 kV and 20 mamps under a vacuum of $2x10^{-8}$ Torr. Sample charging was not eliminated by the use of a neutralizer filament, therefore the C_{1s} peak was shifted to 284.6 eV with a corresponding shift for the rest of the spectrum. Atomic percents of the surface elements were calculated from the area under the 1s peaks with a relative error of 5 %. Results are from a sampling depth of approximately 50 Å.

Initial XPS analysis was carried out at IBM Corporation in Endicott, New York by Dr. Luis Matienzo. Again both high and low resolution spectra were obtained in order to make both quantitative and structural determinations. Carbon 1s peaks were not curve fit, however general information was obtained from the shape of the peaks. Film surfaces were not cleaned or altered before analysis.

2.4.4. Gravimetric Analysis

Weight changes of the films were monitored by weighing samples before and after plasma exposure. A Mettler AE 240 balance was used giving weight measurements within $+/- 3 \times 10^{-5}$ g.

2.4.5. Scanning Electron Microscopy (SEM)

SEM (Phillips model 501, RIT, Microelectronic Engineering Department) was used to evaluate any topographical variations in the AQ55 surface as a result of plasma exposure. Each sample was mounted onto a stainless steel post with silver paint. The posts were first heated to approximately 55 ^{o}C for 15 minutes, then a dab of silver paint was placed on

the top of the post. The sample was then placed on top of the paint with the AQ55 surface of interest facing up. The samples were placed into a desiccator under a nitrogen atmosphere overnight to achieve a stable and dry mount. Samples were then gold coated using a Denton Vacuum Desk II sputter coater. The surfaces were coated at 500 mtorr with 40 mamps for 30 to 60 seconds thereby achieving approximately 100 - 200 Å of gold on the surface. Typical conditions used for the micrographs include: magnifications of 5000 X - 20000 X, either 0^{o} or 40^{o} tilt, 15 or 20 kV, and a spot size of 500.

A few SEM photographs were also taken with an Amray 1830 digital SEM at Xerox Corporation by Ken Kemp. These samples were mounted to stainless steal posts with two sided carbon adhesive tape. Samples were gold coated before analysis in a Hummer 5 plasma system for 4 to 5 minutes in the pulse cycle (5 second pulse). Liquid graphite was used to make a conductive path from the post to the sample. Micrographs were taken at either 10000 X or 20000 X at 20 kV, and a 0^{o} tilt.

2.4.6. Differential Scanning Calorimetry (DSC)

The glass transition temperature of the AQ55 ionomer was determined using a Seiko Instruments Differential Scanning Calorimeter (DSC) Model SSC/5200. AQ55 films were cast into aluminum pans at 70 ^{o}C by dispensing 10 µl of the dispersion into the pan every 30 minutes until a dry weight of approximately 5 - 10 mg of AQ55 was achieved. The sample remained at 70 ^{o}C in the Blue M laboratory oven (model SW17TA) overnight to thoroughly dry the sample. Each sample was weighed and crimped shut with an aluminum cover. A temperature program was used where samples were

cooled from 25 °C to -100 °C at 10 ° C/minute, held at -100 °C for 5 minutes and heated to 150 °C at 5 °C/minute. Nitrogen gas was passed over the samples at 200 ml/minute for 20 minutes prior to and during the DSC run. The midpoint glass transition temperatures are reported.

3.0. Results and Discussion

The goal of this research was to fluorinate the surface of AQ55 via a plasma modification. Several plasma parameters were varied to determine which parameters maximized the degree of fluorination while minimizing degradation and/or etching of the AQ55 surface. The plasma parameters of interest included; gas composition, placement of the sample in the chamber, power, and time of exposure. AQ55 films were exposed to both a 5% O_2/10% Ar/85% CF_4 and 10% Ar/90% CF_4 plasma; samples were placed at the cathode either with a quartz plate suspended above, shielding the film surface from the most energetic part of the glow discharge, or without a shield; the two powers examined included 20 W and 50 W; exposure times ranged from 30 seconds to 30 minutes. The following section discusses how each plasma parameter affected the degree of surface fluorination, degradation, and etching. Analysis of the modified and unmodified films was carried out using contact angles, FTIR/MIR, XPS, SEM, and gravimetric analysis. These analytical techniques aided in the determination of changes in surface energy, surface composition, surface topography, and weight changes of AQ55 after modification.

3.1. Differential Scanning Calorimetry Analysis of AQ55

AQ55 membranes were analyzed with DSC to determine the glass transition temperature (Tg) of the membrane, Table 2. Glass transitions were examined for membranes after an air cast, oven cast (dried), and conversion from the Na^+ to the H^+ form. Dipole-dipole bonding, or ion pairing, has been shown to change the bulk characteristics of ionomeric materials.[25] This

effect has been shown to be influenced by the ionomer water content and the charge density of the counter ion. From this analysis no significant difference was found between the glass transition temperatures for the air cast and oven cast/dried membrane. Therefore water content does not appear to have an appreciable affect on the character of AQ55. After conversion to the hydrogen form, a change of approximately 12°C was observed. This is insignificant in comparison to a system where a substantial amount of ion pairing occurs.[25] This suggests that there is no formation of cluster regions within the ionomer matrix. This is a result of steric factors preventing the close approach of the ionic pendent groups in AQ55. If ion pairing was significant, both crystalline and amorphous regions would be created within the membrane. As a result plasma-surface interactions would be different for both regions. Since the character of the AQ55 membrane is not affected by ion pairing, the surface is believed to be homogenous.

Table 2: The glass transition temperatures for AQ55 with high and low water contents and in a H^+ form.

AQ55 "wet"	AQ55 dry	AQ55 H^+
40°C	42°C	55°C

3.2. The Effects of Gas Composition

AQ55 films were cast onto silicon wafers and exposed to both 5% O_2/10% Ar/85% CF_4 and 10% Ar/90% CF_4 plasmas at 50 W, 20 sccm total gas flow, and 450 to 500 mtorr pressure. The AQ55 films were placed at the cathode without the quartz plate shield. Advancing, receding, and sessile drop contact angles were measured using both DMSO and a pH 7 phosphate buffer as contacting solvents. At least three angles were measured on each film and an average was taken. Increases in contact angles were expected from both DMSO and the pH 7 buffer if surface fluorination was successful. The increase in contact angle was expected since fluorocarbon polymers have low surface energies caused by low intermolecular dispersion forces. Therefore, when a drop of a solvent is placed on a fluorocarbon surface, the drop beads up to maximize the lower energy surface area.

Contact angles are commonly used to determine changes in surface energies of solids relative to the contacting liquid's surface tension. Contact angles are dependent upon the surface tensions of the solid and liquid and on the interfacial tension along the solid-liquid boundary. This relationship is described by Young's equation;[26-28]

$$\gamma_{lv} \cos\theta = \gamma_{sv} - \gamma_{sl} \qquad (4)$$

where θ is the contact angle, γ_{sv} is the solid surface tension, γ_{sl} is the solid-liquid interfacial surface tension, and γ_{lv} is the liquid surface tension. The angle is also influenced by the roughness factor (r) which is the ratio of the actual surface area to that of a smooth surface with the same geometric dimensions (Equation 5).[26]

$$r \cos \theta_{true} = \cos \theta_{rough} \quad (5)$$

A rough surface will reduce wettability further when the contact angle on the smooth surface is above 90° and will decrease the contact angle when the smooth surface already has a contact angle below 90°.[27] Surface topographical changes that have dimensions < 0.1μm are not expected to affect contact angle measurements.[28] Equation 5 is idealistic and that roughness is not adequately described by the roughness factor r. Two surfaces with the same roughness factor will give totally different behavior if the roughness is in the form of parallel grooves on one surface and in the form of random etching on the other. Typically both advancing (θ_A) and receding (θ_R) angles are measured on rough surfaces and the average ($0.5 (\theta_A + \theta_R)$) is assumed to be near the equilibrium contact angle.[27]

Sessile drop and advancing contact angles for films exposed to the $O_2/Ar/CF_4$ plasma are plotted as a function of exposure time in Figure 18. Sessile drop angles are plotted separately from advancing angles and the contact angles for a bare SiO_2 surface are noted in Table 3. Initially only the sessile drop method was performed using only DMSO as the contacting solvent. Sessile drop angles were found to increase from 23° to 36° after exposing AQ55 to the $O_2/Ar/CF_4$ plasma for 2 minutes. Beyond 2 minutes exposure, the contact angles decreased to values obtained on an unmodified AQ55 surface. This decrease indicated that the surface energy increased with exposure time and/or the surface was being roughened by plasma exposure. Oxygen radicals produced in the plasma react with the polymer surface to form free radicals, carbon-oxygen functionalities, and fragmented chain ends.

This increases the surface reactivity and therefore the surface energy relative to the bulk polymer.

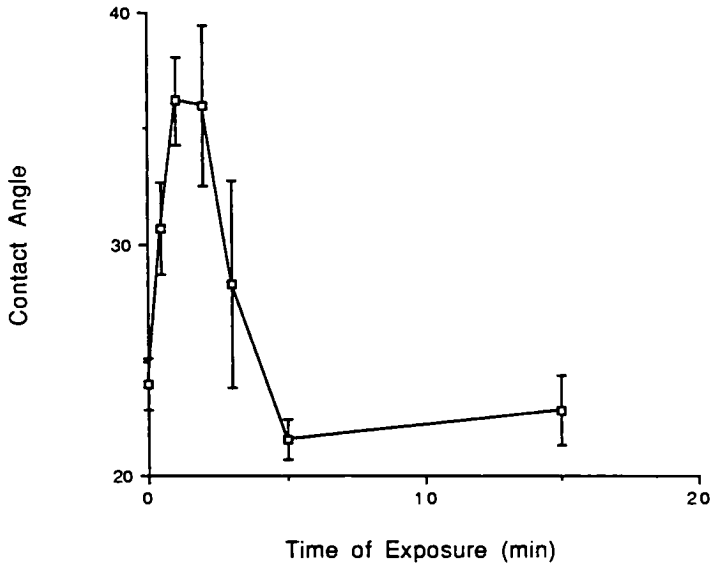

a)

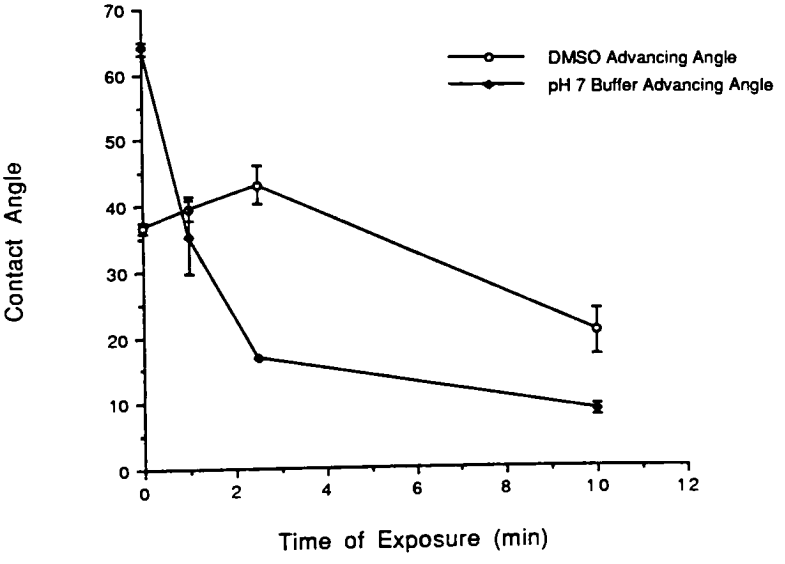

b)

Figure 18: a) Sessile drop and b) advancing contact angles as a function of exposure time for AQ55 surfaces modified with a 50W, 5% O_2/10% Ar/85% CF_4 plasma. DMSO and a pH 7 phosphate buffer were used as contacting angle solvents. The pH 7 buffer was only used for advancing angle measurements.

Table 3: DMSO and pH 7 buffer contact angles measured on a bare Si wafer.

Bare Silicon Wafer	Advancing Angle	Receding Angle	Sessile Drop Angle
DMSO	0^o	0^o	0^o
pH 7 buffer	22^o	22^o	15^o

In order to determine if the decrease in contact angle was a result of surface roughening or oxidation, SEM was used to analyze the surface topography of both unmodified and plasma modified membranes. SEM micrographs were evaluated for an unmodified AQ55 surface and of 5% O_2/10% Ar/85% CF_4 plasma modified AQ55 surfaces after 1, 2.5, and 10 minutes of plasma exposure (Figure2 19 and 20). After 1 minute of plasma exposure the surface structure appears to be similar to the unmodified surfaces with 10,000x magnification (Figure 19). After 2.5 and 10 minutes of exposure the surface appears roughened (Figure 20). This surface damage is uniform and intensifies with time of plasma exposure.

The increase in surface roughness correlates to the decrease in sessile drop and advancing contact angles observed for membranes plasma modified for 2.5 minutes or more. The possibility also exists that the surface energy is increasing because of surface oxidation. Calculation of the equilibrium contact angles eliminates the affect of surface roughness on the measured angle. Since receding angles were not measured at this time, equilibrium contact angles were not calculated for these samples. However the equilibrium contact angles typically follow the same trend as the advancing

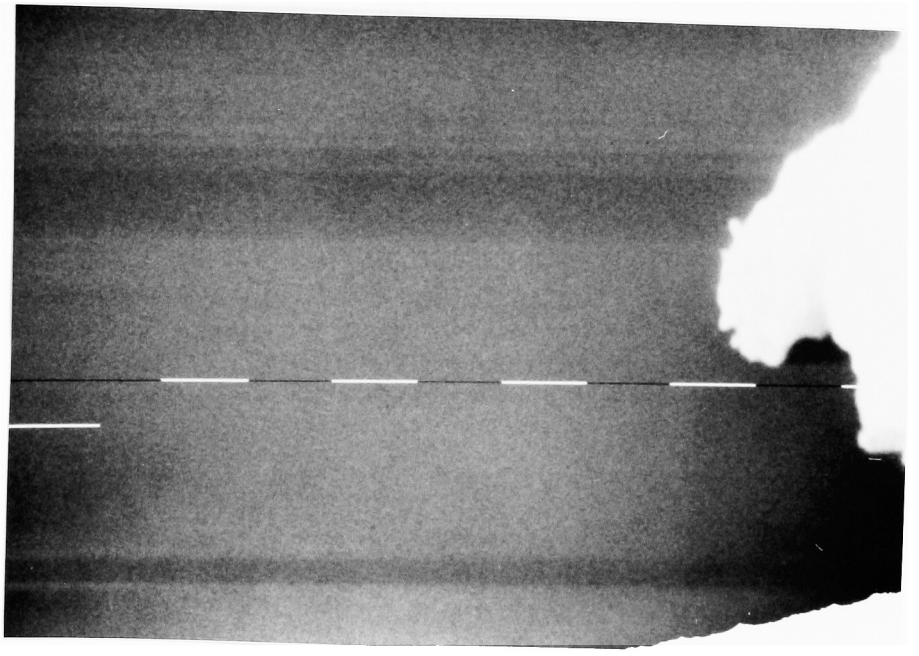

a) Unmodified AQ55 at 10,000 x

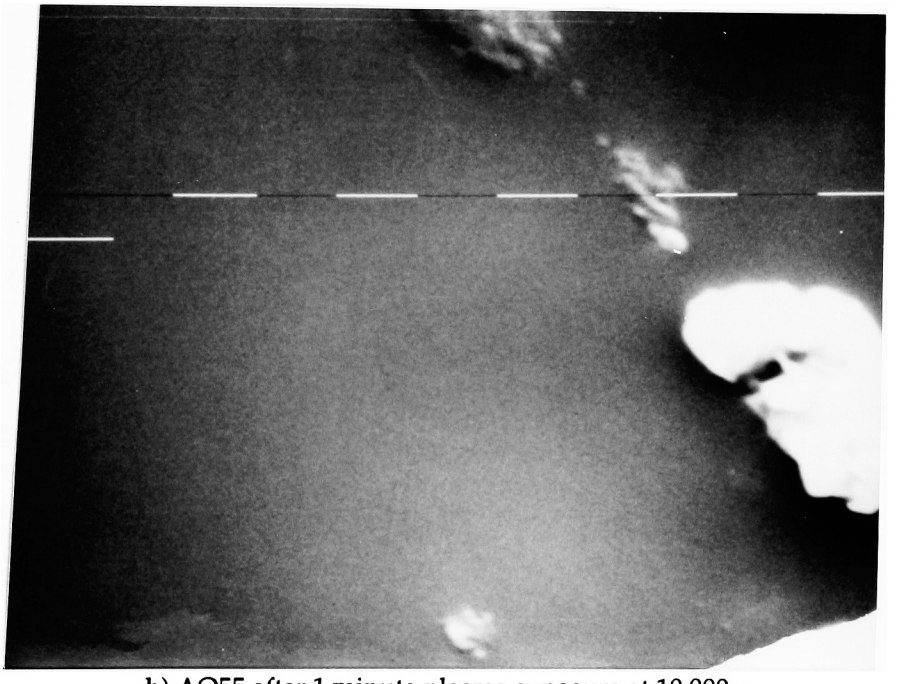

b) AQ55 after 1 minute plasma exposure at 10,000 x.

Figure 19: SEM micrographs of the AQ55 surface a) unmodified, and after b) 1 minute exposure to a 50W, 5% O_2/10% Ar/ 85% CF_4 plasma while at the cathode.

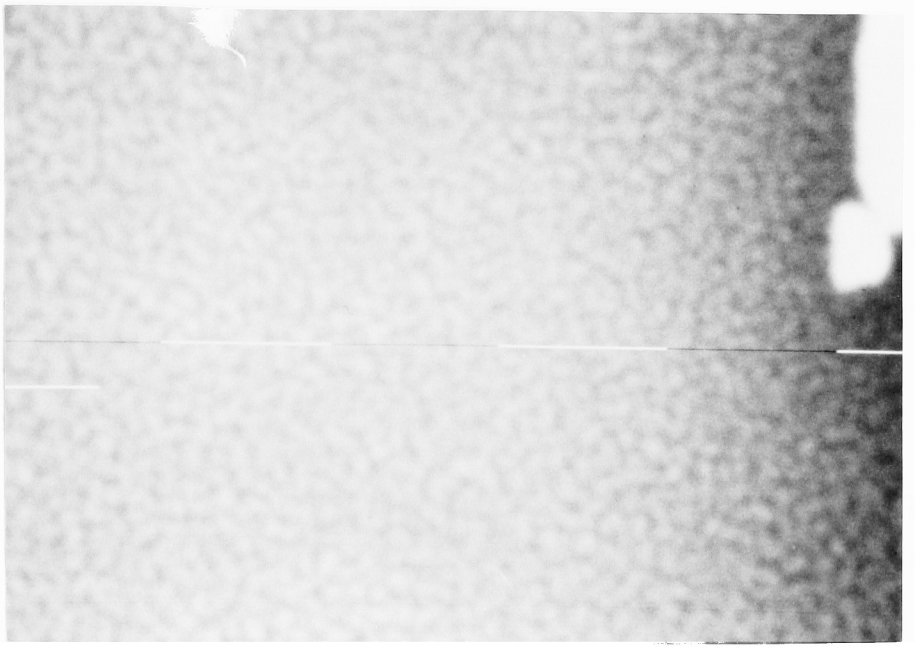

a) AQ55 after 2.5 minutes plasma exposure at 20,000 x.

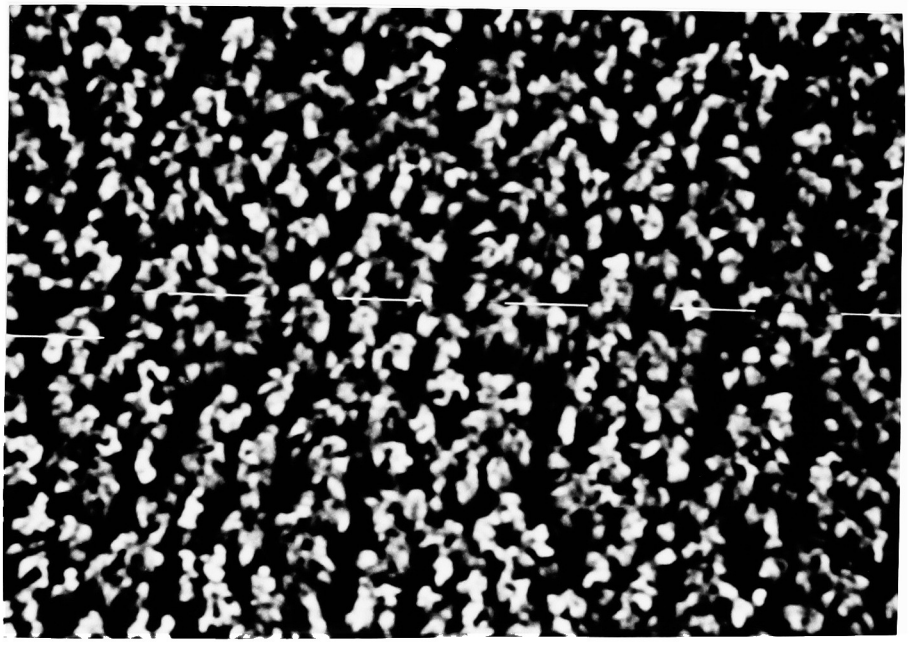

b) AQ55 after 10 minutes plasma exposure at 10,000 x.

Figure 20: SEM micrographs of the AQ55 surface after a) 2.5 minutes and b) 10 minutes of exposure to a 50W, 5% O_2/10% Ar/ 85% CF_4 plasma while at the cathode.

angles. Therefore, since the advancing angles decrease with exposure time, it is assumed that the AQ55 surface increases in surface roughness as well as surface energy upon exposure to the oxygen containing plasma.

Contact angle data for AQ55 surfaces exposed to a 10% Ar/90% CF_4 plasma at 50 W, 20 sccm, and 450 mtorr is plotted in Figure 21 as a function of exposure time. The quartz plate shield was not used for this set of experiments. Under these plasma conditions, a uniform increase in sessile drop and advancing contact angles was observed after all three exposure times for both solvents. This indicates that the elimination of oxygen from the gas feed aided in lowering the surface energy of the AQ55 surface as would be expected for a fluorinated surface. From this data, exposure times between 30 seconds and 10 minutes do not appear to have a significant affect on the modified AQ55 surface energy.

The SEM micrographs of AQ55 surfaces exposed to the Ar/CF_4 plasma for 0.5, 2.5, and 10 minutes are shown in Figure 22 and 23. An increase in surface roughness was observed for times greater than 2.5 minutes of exposure. This explains the slight drop in the pH 7 buffer advancing contact angle at 2.5 minutes of exposure.

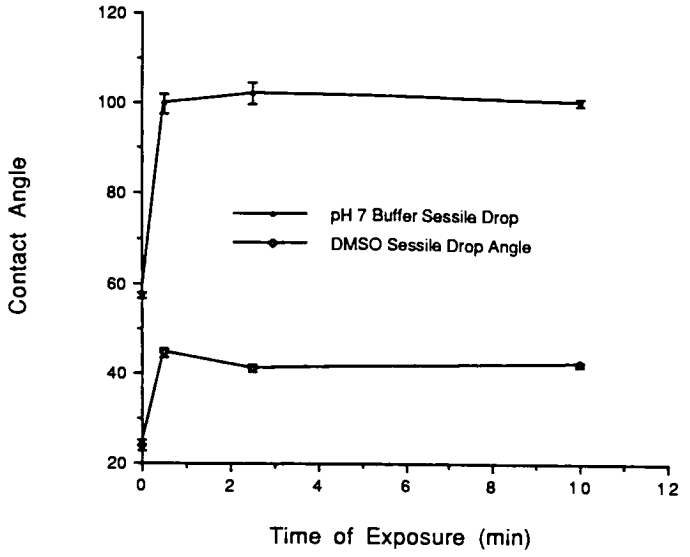

a)

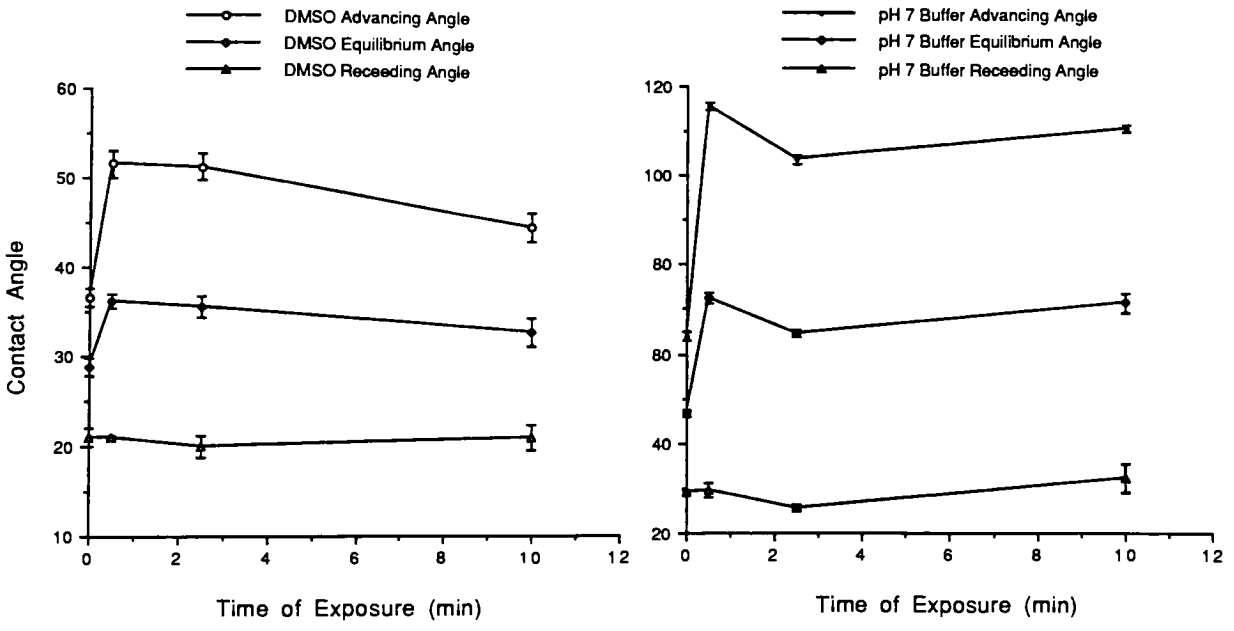

b)

c)

Figure 21 a) Sessile drop and equilibrium contact angles as a function of exposure time for AQ55 surfaces modified with a 50W, 10% Ar/90% CF_4 plasma. Both b)DMSO and a c)pH 7 phosphate buffer were used as contacting angle solvents.

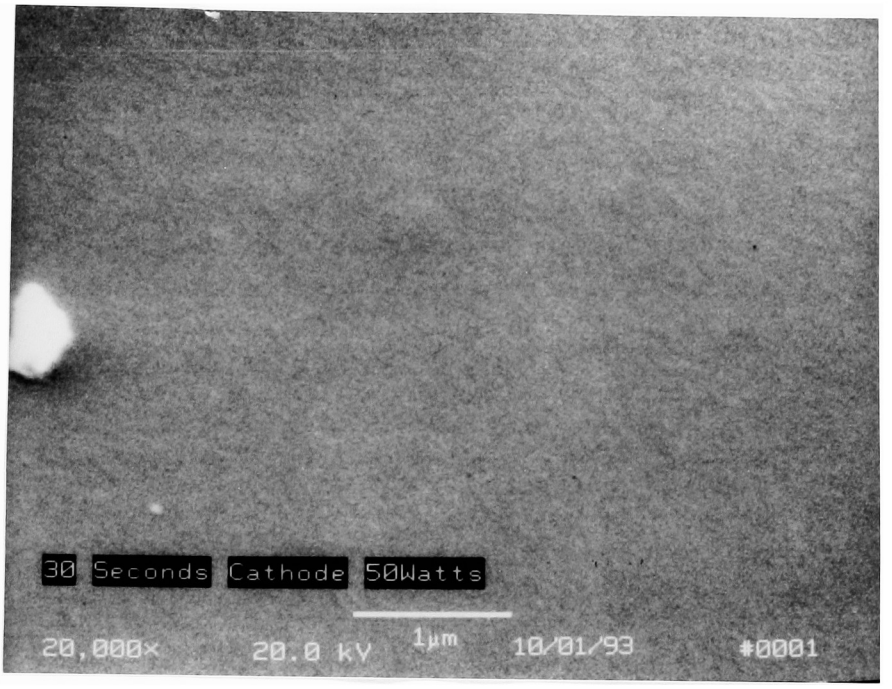

a) AQ55 after 30 seconds of plasma exposure at 20,000 x.

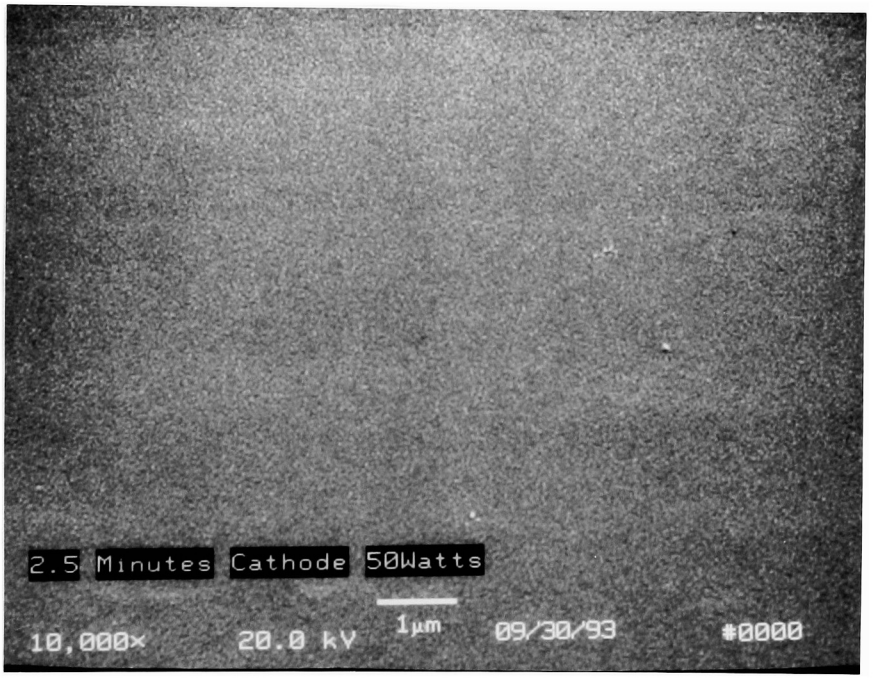

b) AQ55 after a 2.5 minute plasma exposure at 10,000 x.

Figure 22: SEM micrographs of the AQ55 surface after a a) 0.5 minute exposure, b) 2.5 minute exposure, and c) a 10 minute exposure to a 50W, 10% Ar/90% CF_4 plasma while at the cathode.

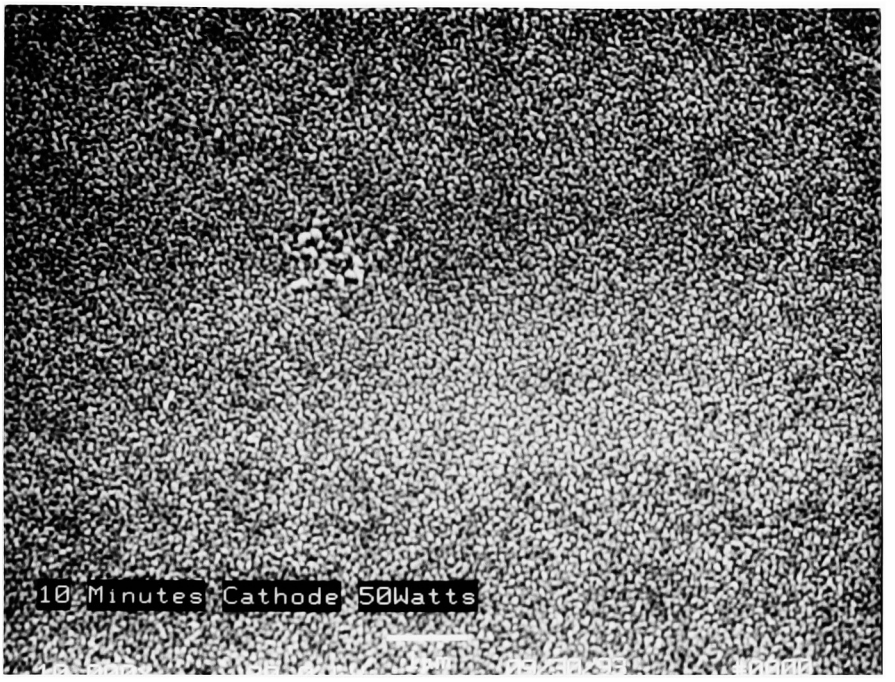

Figure 23: SEM micrographs of the AQ55 surface after a 10 minute exposure to a 50W, 10% Ar/90% CF_4 plasma while at the cathode (10,000 x).

Samples were weighed before and after plasma modification to estimate if a significant weight loss occurred as a result of etching. Measured weight changes are shown in Table 4 for both $O_2/Ar/CF_4$ and Ar/CF_4 plasma modified AQ55 membranes. Generally, the presence of oxygen in the gas feed produced a larger and more rapid weight loss than the Ar/CF_4 plasma. Therefore, it appears that the removal of surface material through chemical etching was produced by reactions of oxygen with the AQ55 surface molecules. This is continued evidence that the presence of oxygen in the gas feed is one factor which aids in producing increased surface energy, and etching.

Table 4: Weight losses for AQ55 samples exposed to both $O_2/Ar/CF_4$ and Ar/CF_4 plasmas at 50W. Sample were placed at the cathode without the quartz plate shield.

Time of Exposure (minutes)	5% O_2/10% Ar/85% CF_4 weight change (g)	10% Ar/90% CF_4 weight change (g)
0.5	---	0.0
1	-6×10^{-5}	0.0
2.5	-5.4×10^{-4}	0.0
10	-3.0×10^{-4}	1.1×10^{-4}

FTIR/MIR analyses of unmodified, $O_2/Ar/CF_4$ and Ar/CF_4 plasma modified films were used to determine the type of chemical functionalities produced at the AQ55 surface after plasma modification. The IR absorbance spectrum of the unmodified film was subtracted from the spectrum of the modified film. Differences in the spectrum were presumed to be directly caused by changes in surface functionalities after plasma exposure.

Infrared absorption band assignments for carbon-oxygen and carbon-fluorine type functionalities are shown in Table 5.[18] The wavelength at which general increases and decreases in absorbtion were observed after both $O_2/Ar/CF_4$ and Ar/CF_4 plasma modifications are shown in Table 6. Both gas compositions resulted in loss of carbonyl (C=O), ether/ester (C-O), and the aliphatic carbon functionalities. The decrease in these absorbance bands are an indication of the loss of carbonyl, ether, and aliphatic carbon functionalities possibly through an alkoxy degradation (Figure 5 page 12) and/or etching. The ether C-O bonds are the weakest bonds in the AQ55 polymer backbone and therefore are the most likely positions of chain scissioning. Bands at 747 and 765 cm^{-1}, assigned to CF_3 or amorphous

Table 5: Infrared band assignments for common carbon-oxygen are carbon-fluorine type functionalities. [18]

Wave number	Assignment	Relative intensity
650	CF_2 wagging	w
740	"amorphous" PTFE	s
980	CF_3	m
1030	CF	m
1050	CF in CF_2	m
1070	CF	m
1160	CF_2 symmetric stretch	vs
1220	CF_2 asymmetric stretch	vs
1340	CF stretch	s
1450	CF_2 asymmetric stretch	sh
1725	C=O stretch	s
1780	C=C stretch	s
1850	C=O stretch	s
3555	O−H stretch	w

poly(tetrafluoroethylene) (PTFE), were observed after exposure of films to both gas compositions. However, the fluorocarbon bands were not observed after short times of exposure because of the sensitivity limitations of the MIR cell. When oxygen was eliminated from the gas feed the PTFE/CF_3 bands appeared after only 1 minute of exposure. With oxygen in the gas feed the PTFE/CF_3 bands were not observed until after 5 minutes of exposure. This indicates that the presence of oxygen is inhibiting the rate of fluorination. According to the proposed fluorination mechanism (Figure 5, page 12), the fluorination rate drops since reactive fluorine species must compete with oxygen for sites on the AQ55 backbone.

Table 6: The infrared band assignment at which increases or decreases in % transmission were observed after exposure to both $O_2/Ar/CF_4$ and Ar/CF_4 plasmas.

5% O_2/10% Ar/85% CF_4 50W at Cathode

Decreases in Absorbance (cm^{-1})	Increases in Absorbance (cm^{-1})	Assignment
1713	—	C=O
1224	—	C-O
725	—	CH_x
—	762	CF_3 / amorphous PTFE

10% Ar/90% CF_4 50W at Cathode

Decreases in %Transmission (cm^{-1})	Increases in %Transmission (cm^{-1})	Assignment
1730	—	C=O
1228	—	C-O
725	—	CH_x
—	747, 765	CF_3 / amorphous PTFE

Problems occurred with the FTIR/MIR analysis when the spectra of the AQ55 membranes were significantly affected by the rubber bumpers from the Perkin Elmer MIR accessory. Aluminum foil was used to cover the rubber bumpers to maximize the reflectance of the beam and minimize any absorbance by the rubber.

Elemental concentrations of carbon, oxygen, fluorine, and sodium found at the surface of AQ55 unmodified and after a 1 minute exposure to a 50 W $O_2/Ar/CF_4$ plasma were determined using XPS (Table 7). The oxygen to carbon ratio (O/C) is also listed in Table 7 to illustrate how the chemical structure of AQ55 changes after plasma modification. An increase in the O/C ratio relative to the unmodified AQ55 O/C ratio would indicate that AQ55

was oxidized during plasma exposure. A lower O/C ratio would indicate either that there was a loss of oxygen or addition of carbon during plasma exposure. The addition of carbon could be the result of CF_x type functionalities grafting to the AQ55 surface.

Table 7: Elemental concentrations of C, O, and F detected on unmodified AQ55 and AQ55 modified with a 50W, $O_2/Ar/CF_4$ plasma for 1 minute. Analysis by XPS.

Sample	Atomic %C	Atomic %O	Atomic %F	Atomic %Na	O/C
AQ55 unmodified	74	26	0	0	0.35
AQ55 after 1 min plasma	41	19	31	9	0.47

The XPS data shows significant evidence of both fluorination and oxidation after the one minute exposure to a 50 W, 5% O_2/10% Ar/85% CF_4 plasma. A total of 31% atomic fluorine was achieved at the AQ55 surface after exposure to the $O_2/Ar/CF_4$ plasma. This increase in fluorination corresponds to the increased sessile drop contact angles after a 1 minute plasma exposure. An increase in the oxygen to carbon ratio (O/C) from 0.35 to 0.47 was observed after plasma exposure which indicates that oxidation also occurred. Therefore surface oxidation is a factor which would cause the increase in surface energy indicated by the contact angle results beyond 2 minutes of exposure. Surface fluorination of AQ55 was achieved by exposure to a $O_2/Ar/CF_4$ plasma. This is conclusive evidence that the presence of

oxygen in the gas feed aided in increasing the surface energy and wettability of the AQ55 surface through surface oxidation.

An increase in the sodium concentration on the AQ55 surface was also found after $O_2/Ar/CF_4$ plasma modification. The absence of sodium on the unmodified AQ55 surface could possibly be a result of residual water occluded at the film center causing the sodium sulfonate groups to align towards the film center rather than the film surface. Two factors that possibly caused the increase in sodium concentration after plasma modification include; exposure to temperatures above the Tg, and etching. Increased molecular mobility above the Tg could have allowed for the realignment of sodium sulfonate groups towards the film surface. Another explanation may be that material was being removed from the surface during plasma exposure thereby exposing the sodium ions. If this is true then the sodium concentration can be a good indicator of the degree of etching, unless sodium ions are also removed with further exposure.

High resolution XPS spectra allowed chemical structural determinations to be made based on the shape and shift in the C 1s peak. Carbon 1s (C 1s) binding energies for common fluorocarbon and carbon-oxygen functionalities as determined by XPS analysis are shown in Table 8. As the number of electronegative atoms bonded to a carbon atom increases, the binding energy of the carbon 1s electron increases. The entire C 1s peak can be deconvoluted into separate contributions so that the quantification of the separate carbon functionalities is possible.

Table 8: Carbon 1s binding energies for different functionalities.[7,18]

$\underline{C}F_3$	293.0 - 294.0 eV
$\underline{C}F_2$	290.5 - 292.2 eV
$\underline{C}F\text{-}CF_n$	290.0 eV
$\underline{C}F$	288.5 - 289.5 eV
$\underline{C}OO$ and $\underline{C}OC$	288.6 eV
$\underline{C}{=}O$	288.1 eV
$\underline{C}F$ and $\underline{C}\text{-}CF_n$	287.0 eV
$\underline{C}O$	286.4 - 287.5 eV
$CF_2\text{-}\underline{C}H_2$	285.8 eV
$\underline{C}H_n$	285.0 eV
$\underline{C}H_2$	284.5 - 285.0 eV

The C1s peaks for both the unmodified AQ55 film and a $O_2/Ar/CF_4$ modified film are shown in Figure 24. These peaks were not deconvoluted (curve fit) into individual contributing peaks, however general shifts are apparent. The C1s peak for the unmodified film has the most significant contribution centered at 285 eV attributed to CH_2 type functionalities. A slight shoulder is observed at 286 eV attributed to ether (C-O) functionalities. The carbonyl C=O and carboxylic acid COO functionalities are denoted by the second peak at 288.5 eV. After plasma exposure, the increase in the full width at half the maximum (FWHM) height of the peak at 285 eV is indicative of an increase in the number of contributing functionalities to this peak (Figure 24 b). Therefore, the additions of O and F atoms to carbons in the AQ55 backbone contribute to this peak widening. An increase in the peak intensity is observed between 287 and 291 eV as the result of the addition of fluorine and oxygen to the surface. However, the ratio of the 285 eV peak

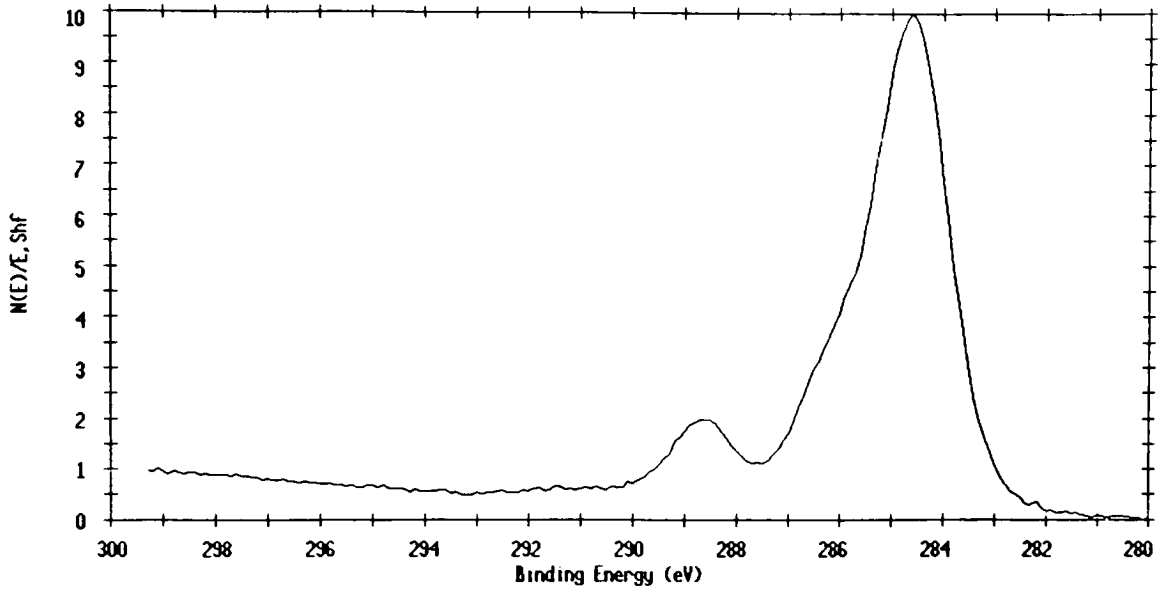

a)

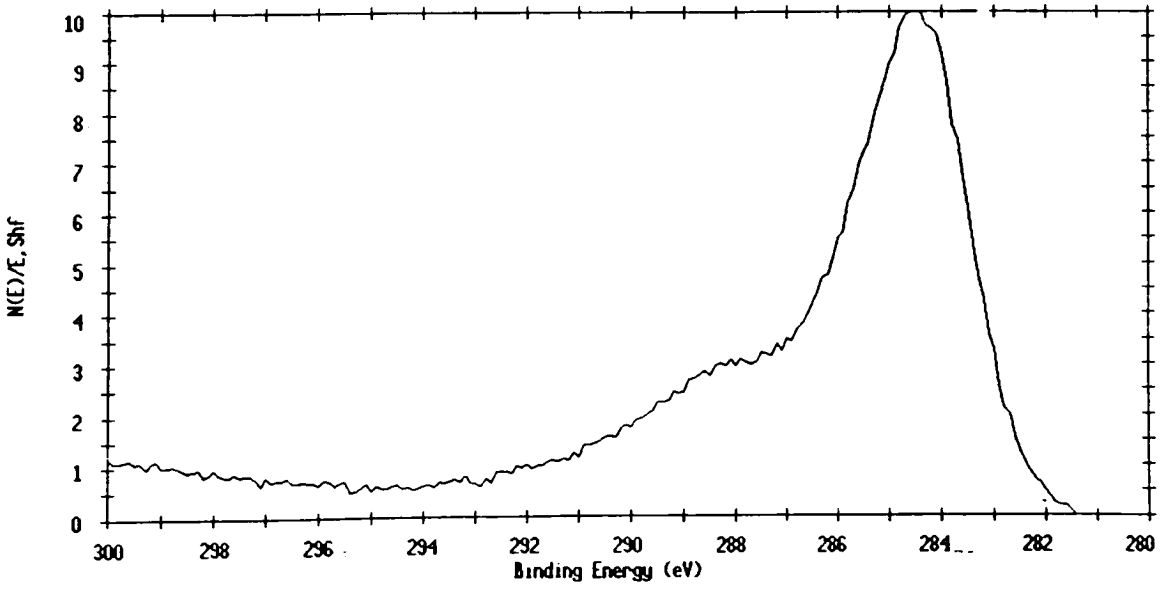

b)

Figure 24: C1s spectra for a) unmodified AQ55 and b) $0_2/Ar/CF_4$ plasma modified AQ55. (1 minute exposure)

height to the 288.5 eV peak height was still rather large. This implies that only a small conversion of the hydrocarbon functionalities to fluorocarbon or carbon-oxygen functionalities was achieved within the 50 Å depth of analysis.

Carbon, oxygen, and fluorine atomic percents detected on the AQ55 surfaces after exposure to a 50W, 10% Ar/90% CF_4 plasma are plotted in Figure 25 as a function of exposure time. The fluorine atomic percent increased to 24% after 30 seconds of exposure and remained constant at approximately 25% for up to 10 minutes exposure. The oxygen to carbon ratio (O/C) after 30 seconds of exposure was 0.32 and was very close to the O/C ratio of the unmodified film at 0.35. An average O/C ratio of 0.26 was

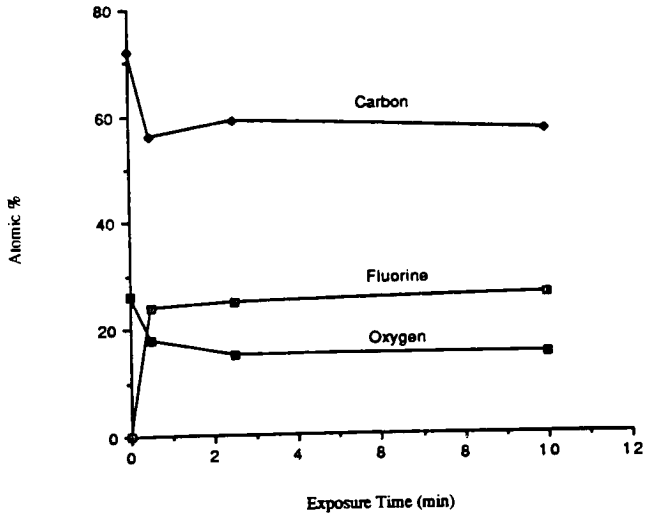

Figure 25: The atomic percents of carbon, oxygen and fluorine detected at the AQ55 surface after exposure to a 50W, 10% Ar/90% CF_4 plasma for 0.5, 2.5 and 10 minutes exposure. Samples were placed at the cathode.

found at 2.5 and 10 minutes of exposure. Therefore the number of carbons relative to the number of oxygen atoms was increased at the surface when oxygen was removed from the gas feed. This may either be the result of loss of oxygen or the addition of carbon through grafting of CF_x functionalities to the surface at radical sites. As discussed in references 13 and 17, the addition of oxygen to the gas feed drastically reduced concentrations of CF_3 and CF_2 radicals in the plasma and increased atomic fluorine concentrations. Therefore without oxygen present, the probability of CF_3 and CF_2 radical reactions with the AQ55 surface is higher. This is evidence that the decreased O/C ratios are the result of the addition of carbon through the grafting of CF_x species.

The C 1s spectra for AQ55 films exposed to a 10% Ar/90% CF_4 plasma at 50 W are shown in Figure 26. The spectra for 0.5, 2.5, and 10 minute exposures are shown. The peaks were curve fit with six or seven contributions. Difficulties arise in labeling specific functional contributions since both carbon-oxygen and carbon-fluorine functionalities have similar and sometimes identical chemical shifts in binding energy. Therefore since both carbon-oxygen and carbon-fluorine functionalities are present, many of the peaks are non-unique therefore there is a degree of uncertainty in the energy locations and number of peaks necessary to produce a reasonable curve fit. This technique cannot distinguish between carbon-oxygen and carbon-fluorine functionalities at similar binding energies, however the previous quantitative analysis shown in Figure 25 indicates that fluorocarbon functionalities should predominate.

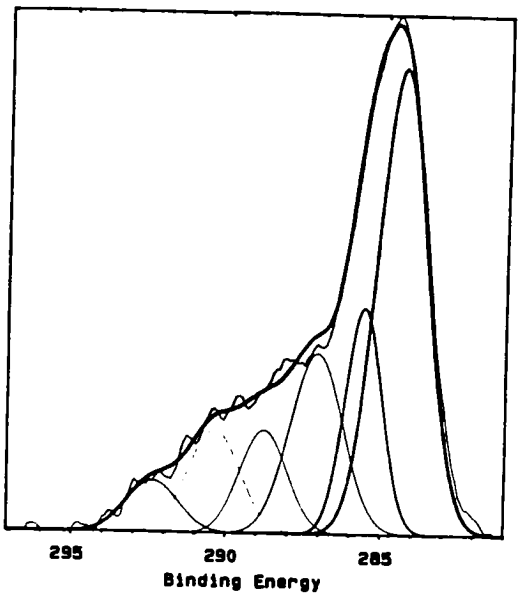

a)

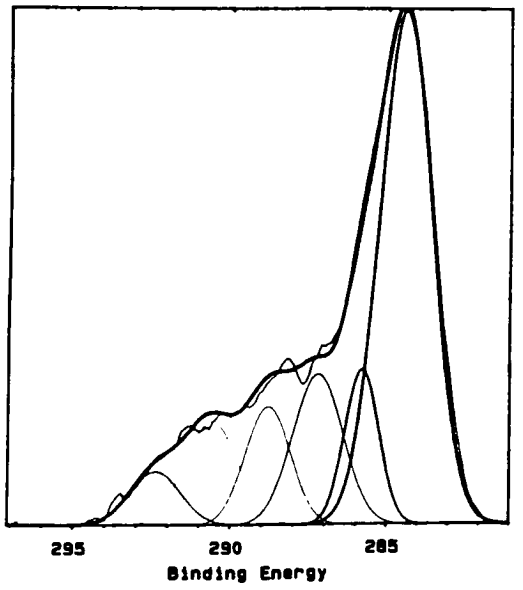

b)

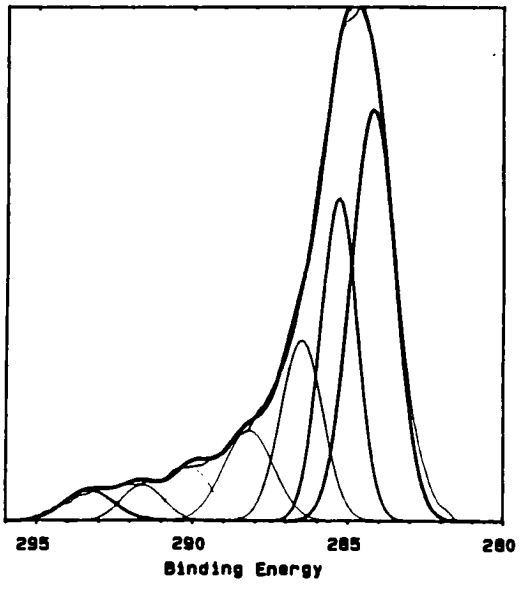

c)

Figure 26: The C 1s spectra for AQ55 surfaces modified with a 50W, 10% Ar/90% CF_4 plasma for a) 0.5, b) 2.5 and c) 10 minutes at the cathode.

The approximate percent contribution of each of the contributing C 1s peaks are listed in Table 9 along with the C-O and C-F functionalities unique to the given binding energies. Quantitative analysis of the specific functionalities is not possible since each peak may not be unique to a single functionality. The 30 second and 2.5 minute exposures show a significant increase in the CF_3 and $C\text{-}CF_2$ functionalities with exposure time. However,

Table 9: The binding energy, percent contribution, and the assigned carbon-oxygen and carbon-fluorine functionalities for each of the contributing C1s peaks for the Ar/CF_4 plasma modified surfaces.

Exposure Time (min)	282 -284 eV % CH_2	285 -286 eV %C-CO %C_nF	287 eV % C-O %C_nF	287 eV %C-O %C_nF	289 eV %C=O %C_nF	291 eV %COO^- %$C\text{-}CF_2$	292 eV %CF_3
0.5	42	15	17	9	10	—	5
2.5	51	10	14	10	10	—	5
10	38	25	16	9	4	3	3
AQ55 Blank	72	—	—	20	7	—	—

after 10 minutes the CF_3 and CF_2 contributions decrease, as a result of the surface etching/degradation observed in the SEM micrographs. The atomic percents fluorine remain constant with time of exposure, however these plots indicate that the type of fluorination changes with time. Etching of the AQ55 surface would continuously produce a new surface which is modified and removed with time of plasma exposure. Therefore the type of chemical functionalities found at the AQ55 surface are changed with exposure time.

The strongest contribution in the C1s spectra after Ar/CF_4 plasma modification is attributed to CH_2 type bonding. This indicates that

fluorination did not extend into the depth of XPS analysis, which is approximately 50 Å. This may occur since the depth of fluorination is not allowed to increase because of the surface degradation which continually exposes a new surface with time of exposure. Therefore, the fluorocarbon functionalities at the surface are a small percentage of the analysis depth and CH_2 functionalities still dominate.

Three factors that contribute to the surface etching and/or degradation observed include; high energy ion bombardment, the presence of oxygen in the plasma, and exposure to increased temperatures. Ion bombardment has been suggested to form free radical sites on the polymer backbone.[20] These radicals are highly reactive and promote chain scissioning. Free radicals may also react with oxygen promoting reactions such as the alkoxy degradation.[17] When chain scissioning occurs to a large enough degree, a large number of chain ends are formed at the surface, and/or low molecular weight fragments are chemically removed. The consequence would be a degraded and/or chemically etched surface. Oxidation also produces polar and reactive carbon-oxygen functionalities at the surface which increase the surface energy relative to the bulk. These consequences are depicted by the AQ55 weight loss, increased surface roughness, increased O/C ratio and decrease in contact angles after exposure to the oxygen containing plasma.

After elimination of oxygen from the gas feed, contact angles increased, and changes in surface topography were still observed. This indicates that the increased surface energy resulting from the oxygen containing plasma was not solely dependent upon the change in surface topography. For the Ar/CF_4 plasmas, care was taken to backfill the plasma

chamber with argon gas before the experiment so as to eliminate atmospheric oxygen from the chamber. Trace amounts of oxygen contaminates may have been present in the gas feeds and complete elimination of atmospheric oxygen may not have been achieved such that alkoxy degradation was not eliminated. Samples were also exposed to the most energetic part of the glow discharge where high energy ion bombardment was highly probable. Therefore, after elimination of oxygen from the gas feed, the degraded surface was most likely a result of ion bombardment initiating ion assisted etching.

Temperatures measured after each of the above experiments are plotted in Figure 27 as a function of exposure time for both the $O_2/Ar/CF_4$

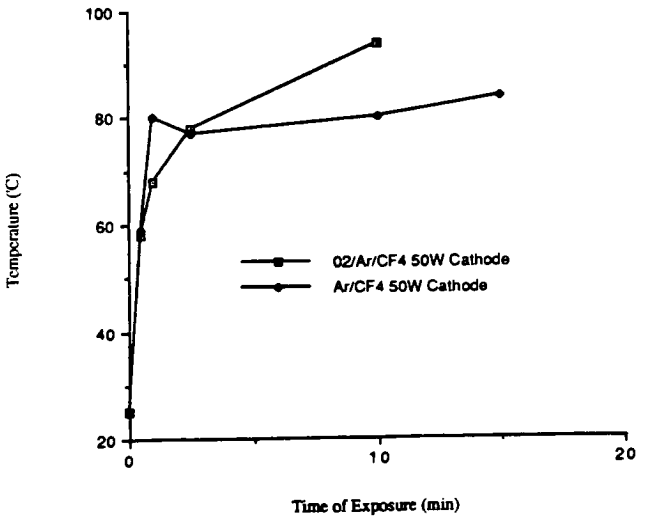

Figure 27: Plot of measured temperatures as a function of time for both $O_2/Ar/CF_4$ and Ar/CF_4 50W plasmas while samples were at the cathode.

and Ar/CF_4 plasmas. Under both gas feed conditions, the temperature increased with exposure time and exceeded the Tg of AQ55 after only 30 seconds of exposure. This increase in temperature aids in depropagation of the polymer chain and therefore is believed to be another factor causing degradation. Depropagation is caused by the increased polymer chain mobility and reactivity above the Tg.

From these results it has been found that elimination of oxygen from the gas feed assists in decreasing the surface energy of AQ55 and increasing the fluorine content on the surface. However, changes in surface topography are still observed because of the exposure to high temperatures, ion bombardment, and trace amounts of oxygen in the gas feed.

3.3. The Effects of The Sample Placement

AQ55 film samples were plasma modified at the cathode surface either with a quartz plate shield approximately 1.2 mm above the samples, or without the quartz plate shield. The following experiments were designed in order to establish the affects the protective shield would have on fluorination and degradation of the ionomer surface.

The DMSO and pH 7 buffer contact angles measured on the AQ55 surface before and after a 50 W, 10% Ar/90% CF_4 quartz plate protected plasma exposure, are plotted in Figure 28 as a function of exposure time. The contact angles measured on samples exposed to the same plasma without the protective quartz plate are shown in Figure 21, page 53. Increases in both the sessile drop and advancing contact angles were not as rapid for the samples

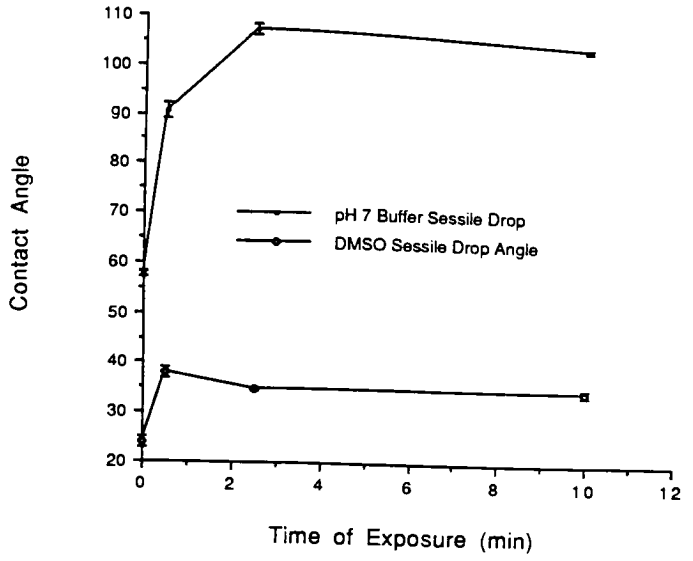

a)

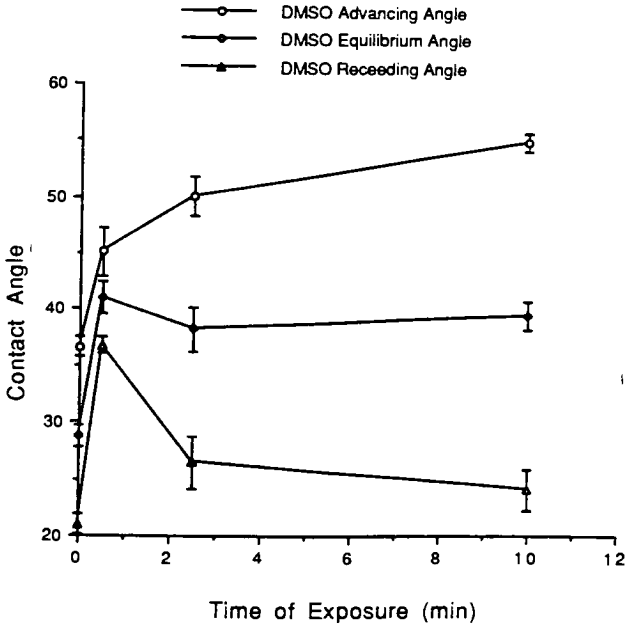

b)

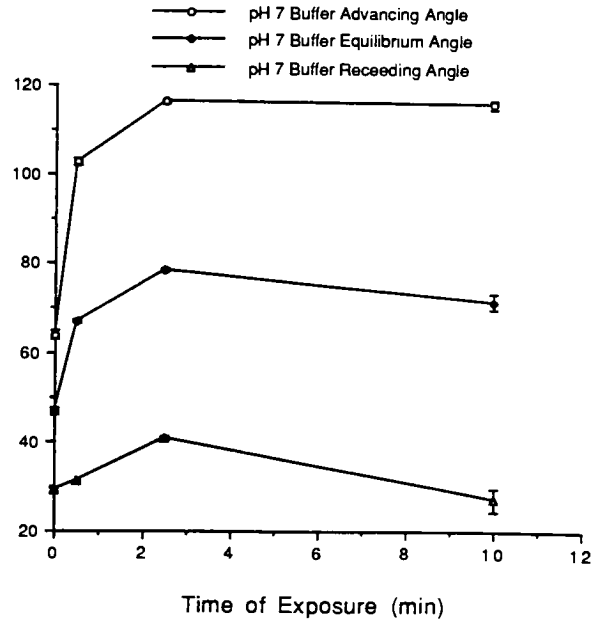

c)

Figure 28: a) DMSO and pH 7 buffer sessile drop contact angles. b) DMSO advancing, receding and equilibrium contact angles. c) pH 7 buffer advancing, receding and equilibrium contact angles. Samples were exposed to a 50W, 10%Ar/90% CF_4 plasma with a quartz plate shield above the samples.

protected with the quartz plate shield. This is a result of the quartz plate shield blocking direct exposure to the reactive species in the plasma and possibly decreasing the effects of ion bombardment. As a result of decreased ion bombardment, the contact angles for the shielded samples did not decrease at 10 minutes of exposure unlike the contact angles for the unshielded samples. Therefore, the quartz plate decreased the rates of fluorination and degradation by removing the sample from the most energetic part of the plasma.

SEM micrographs for shielded samples exposed for 0.5, 10 and 30 minutes are shown in Figures 29 and 30. A smooth surface was observed at 10,000 x even after 30 minutes of exposure. This proved that the protective quartz plate eliminated surface degradation caused by direct ion bombardment. The shield eliminated degradation, however it did not eliminate surface fluorination. This was confirmed by the contact angle data and the results that follow.

Samples exposed to a 50W, 10% Ar/90% CF_4 plasma while shielded with the quartz plate did not show any significant weight loss until after 10 minutes of exposure. A sample exposed for 10 minutes lost 8.0×10^{-5} g. This is similar to the amount lost after 10 minutes of exposure to the Ar/CF_4 plasma without the quartz plate. Therefore the same degree of etching and/or water loss is occurring with and without the quartz plate present. Since samples exposed to the $O_2/Ar/CF_4$ plasma without the quartz plate lost 3.0×10^{-4}g, it is believed that the presence of oxygen is driving the etching mechanism.

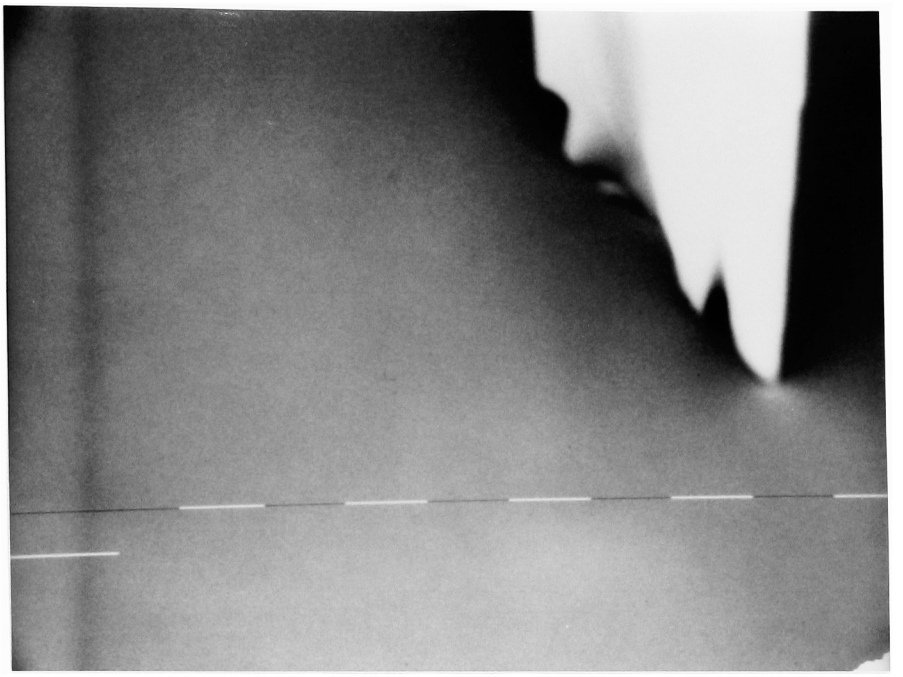

a) AQ55 after 30 seconds of plasma exposure at 10,000 x.

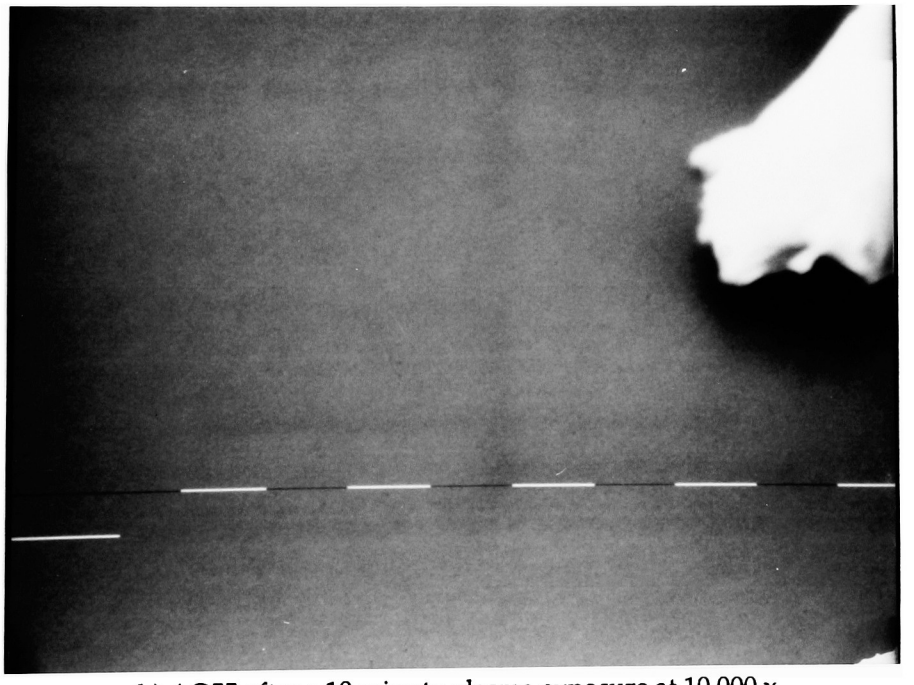

b) AQ55 after a 10 minute plasma exposure at 10,000 x.

Figure 29: SEM micrographs of AQ55 surfaces after exposure to a 50W, 10%Ar/90%CF_4 plasma with the quartz plate shield for a) 0.5 minutes and b) 10 minutes.

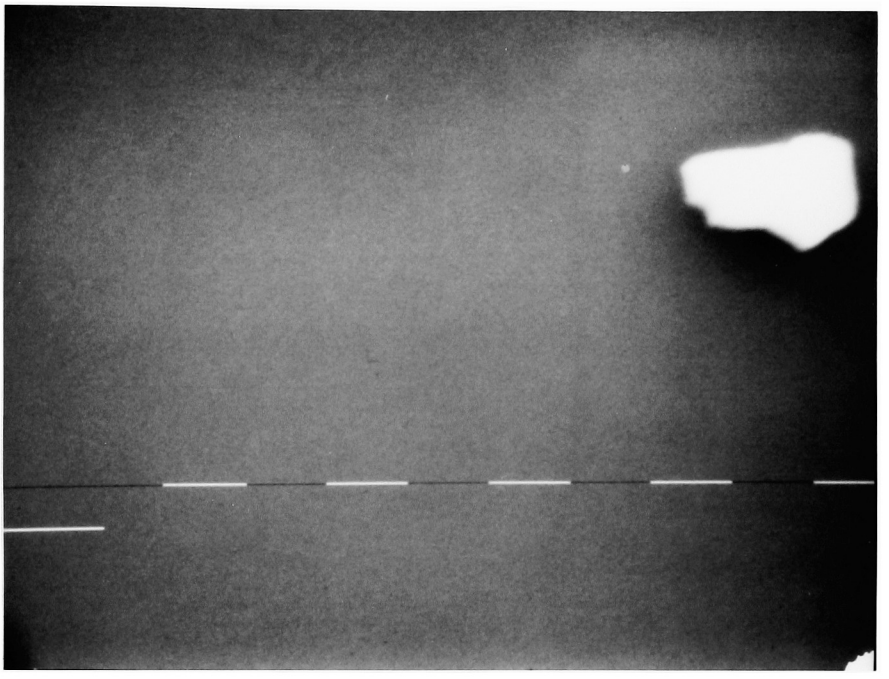

Figure 30: SEM micrograph of AQ55 surface after exposure to a 50W, 10%Ar/90%CF_4 plasma with the quartz plate shield for 30 minutes at 10,000 x .

An experiment was conducted where a sample was exposed to the same Ar/CF_4 plasma for 30 minutes with only half protruded from underneath the quartz plate. After plasma exposure, the AQ55 film was visually examined. The portion of the film which remained under the quartz plate during plasma modification appeared unaltered. The portion which was not covered with the quartz plate sustained topographical damage which was apparent to the naked eye. This indicates that the quartz plate was a significant aid in eliminating surface damage even at long exposure times.

FTIR/MIR analysis of the AQ55 membranes exposed to the 50 W, 10% Ar/90% CF_4 plasma while shielded with the quartz plate did not reveal a loss

of the carbonyl, ester or alkane functionalities at the surface. However, bands at 726 and 625 cm^{-1}, attributed to carbon-fluorine stretches, appeared after 2.5 minutes of exposure. This increase in fluorocarbon functionalities beyond 2.5 minutes exposure correlates to the increases in contact angles observed for the identical surfaces. Also, the FTIR/MIR results are supported by the gravimetric and SEM results which indicate that surface degradation and etching were insignificant.

The temperatures recorded after the 50 W, Ar/CF_4 quartz plate plasma modification are plotted in Figure 31 as a function of exposure time. Temperatures reached with the quartz plate are higher relative to the experiments without the quartz plate. It is possibly a result of the quartz plate acting as a heat sink thereby increasing temperatures near the AQ55 surface and/or that the AQ55 film above the thermocouple wires was

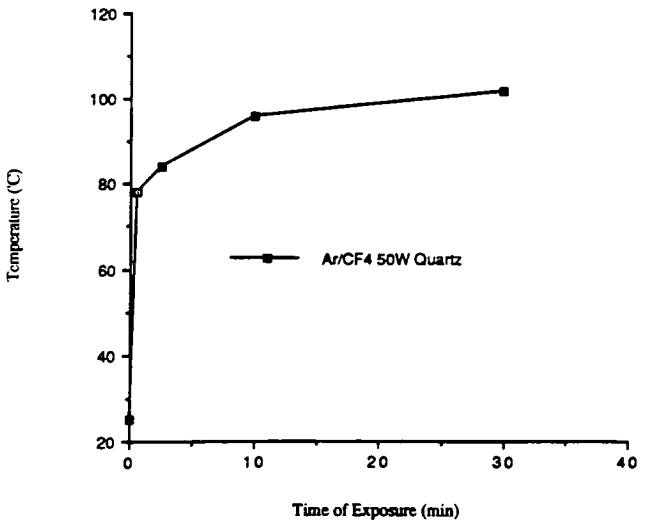

Figure 31 Temperatures recorded after a 50W, 10% Ar/90% CF_4 plasma with the quartz plate shield present. Temperatures are plotted as a function of time of exposure.

degraded as a result of repeated experiments. The temperatures reach 100°C which could be detrimental to the membrane surface. Increased molecular mobility would have been significant since temperatures exceeded the Tg. Also, reaction rates for depropagation of the polymer chain, fluorination, alkoxy degradation, oxidation and etching would be increased. However, there is no evidence of the temperature having a significant effect on surface degradation.

Atomic percents of carbon, oxygen and fluorine detected at the surface of AQ55 after exposure to a 50W, 10% Ar/90% CF_4 plasma with the quartz plate present are plotted as a function of exposure time in Figure 32. The percent of atomic fluorine increased to 56% after only 30 seconds of exposure.

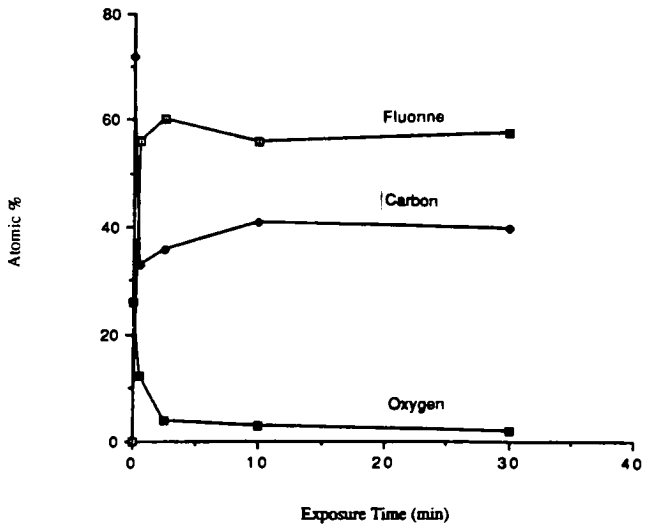

Figure 32: The atomic percents of carbon, oxygen, and fluorine detected at the surface of AQ55 after a 50W, 10% Ar/ 90% CF_4 plasma with the quartz plate shield. Atomic percents were determined by XPS and are shown as a function of exposure time.

This is the highest rate of fluorination achieved for this project. Between 30 seconds and 30 minutes of plasma exposure, the percent atomic fluorine detected at the AQ55 surface remains relatively constant at an average of 58%. The O/C ratio decreases with time of exposure from 0.37 at 30 seconds to 0.05 after 30 minutes. The O/C ratios are plotted in Figure 33 as a function of exposure time. This dramatic decrease in the O/C ratio is assumed to be the result of CF_x species grafting to the AQ55 surface. The O/C ratio also decreased for samples exposed to the Ar/CF_4 plasma without the quartz plate shield, however, the decrease was not as dramatic. The O/C ratio decreased from 0.32 at 30 seconds of exposure to 0.26 between 2.5 and 10 minutes of exposure without the quartz plate. Therefore, the quartz plate shield was effective in increasing fluorination by reducing the effects of ion milling caused by high energy ion bombardment.

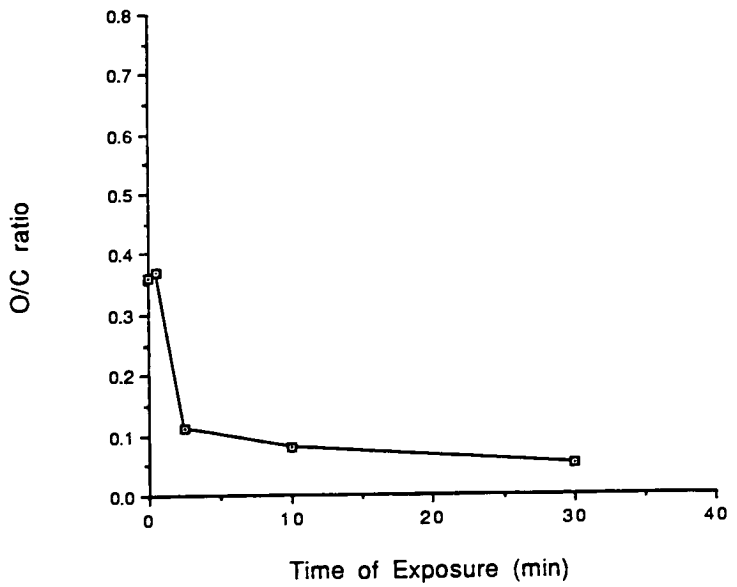

Figure 33: The O/C ratio at the surface of AQ55 after a 50W, 10% Ar/90% CF_4 plasma exposure with the quartz plate. Ratios plotted as a function of exposure time.

Sodium was not detected on any AQ55 sample after a 50 W, Ar/CF_4 plasma exposure using the quartz plate. Previously, 2% atomic sodium was detected on surfaces after the same exposure without the quartz plate. It was suggested that the realignment of the sodium ions towards the AQ55 surface after modification may have resulted from the following; increased molecular mobility at temperatures above the Tg, etching and/or degradation of the AQ55 surface exposing underlying sodium ions. Samples for this 50W Ar/CF_4 experiment experience the highest surface temperatures, however, no increase in sodium content resulted as indicated by XPS analysis. Therefore the realignment of sodium ions to the surface is not a result of elevated temperatures but was more likely a result of degradation of the surface.

A control sample was exposed to a pure argon plasma for 2.5 minutes at 50 W with the quartz plate shield present. One percent atomic fluorine was detected at the AQ55 surface with XPS. The most likely source of the fluorine was from residual CF_X species adsorbed on the chamber wall. The O/C ratio was found to increase from 0.35 on an unmodified surface to 0.47. Therefore, even in the apparent absence of oxygen, oxidation of the surface was possible. This results from the trace amounts of oxygen contaminates in the gas feed, atmospheric oxygen still present at the working pressures or long lived free radicals reacting with atmospheric oxygen once the samples are removed from the chamber.

The C 1s spectra for AQ55 samples modified with a 50 W, 10% Ar/90% CF_4 plasma under the quartz plate and after 0.5, 2.5, 10, and 30 minutes exposure are shown in Figure 34. The C 1s spectra for an AQ55 film after 2.5 minutes exposure to a 50 W pure Ar plasma (with quartz plate) is shown in

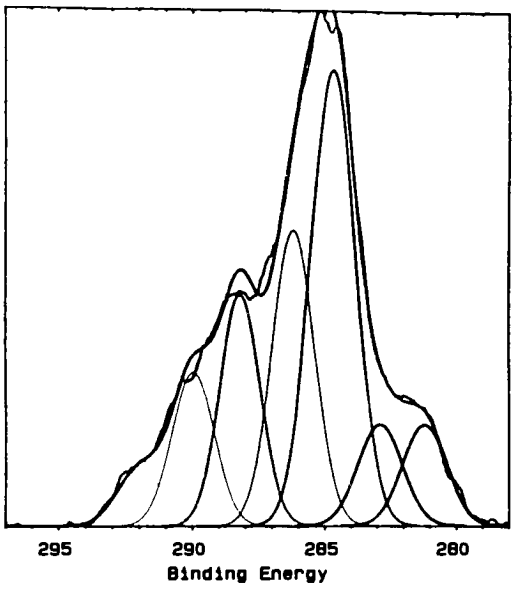

a)

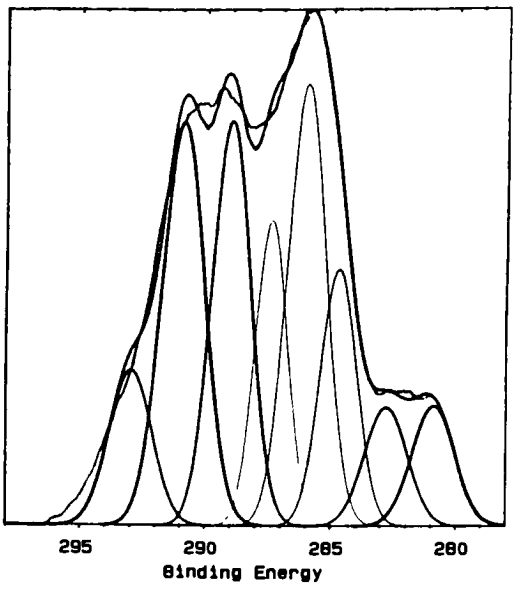

b)

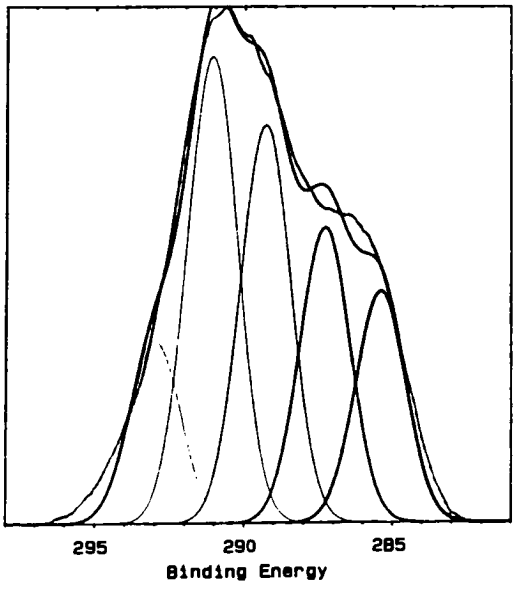

c)

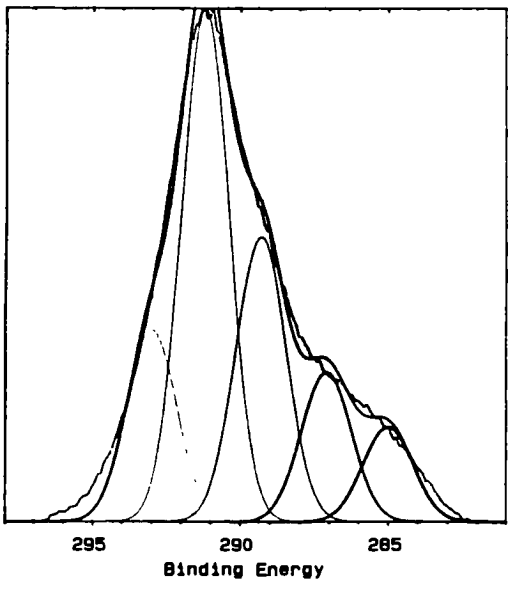

d)

Figure 34: The C 1s spectra for AQ55 samples exposed to a 50W, 10% Ar/90% CF_4 plasma while under a quartz plate and after a) 30 seconds, b) 2.5 minutes, c) 10 minutes, and d) 30 minutes of exposure.

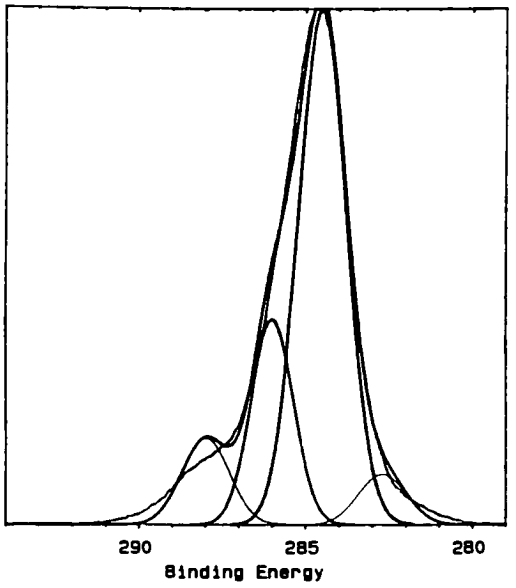

Figure 35: The C 1s spectrum for AQ55 exposed to a 50W, Ar plasma for 2.5 minutes while under the quartz plate.

Figure 35. The control is similar to the unmodified AQ55 C 1s spectra (Figure 24 page 62). Table 10 lists the percent contribution of each peak fit into the C1s spectrum. A slight increase in the peak at 288 eV was observed in the control spectrum, which is attributed to carbonyl carbons. A significant shift in the C1s spectrum to higher binding energies occurs with increased exposure time to an Ar/CF_4 plasma. Under these plasma conditions a notable increase in binding energy is observed after only 30 seconds of exposure. A notable difference can be seen when comparing the C 1s spectra of samples placed at the cathode without the quartz plate (Figure 26 page 65) to samples placed beneath the quartz plate under the same plasma conditions. There is a much more rapid shift from the CH_2 to CF_X type

bonding with a quartz plate shield present. After only 30 seconds exposure to the 50 W, Ar/CF_4 plasma, the percent of CH_2 contributions dropped 23%. Again, since the O/C ratio decreases and the percent fluorine increases with exposure time, the shift to higher binding energies are believed to be predominately from the addition of fluorine and fluorocarbon species to the surface.

Table 10: The binding energy, percent contribution, and the assigned carbon-oxygen and carbon-fluorine functionalities for each of the contributing C1s peaks for the 50W, Ar/CF_4 plasma modified surfaces. Samples were protected by the quartz plate during plasma exposure.

Exposure Time (min)	282 -284 eV % CH_2	285 -286 eV %C-CO %C_nF	287 eV % C-O %C_nF	287 eV %C-O %C_nF	289 eV %C=O %C_nF	291 eV %COO^- %C-CF_2	292 eV %CF_3
0.5	49	—	—	21	16	11	4
2.5	22	—	20	11	18	20	8
10	—	14	—	18	25	29	11
30	—	8	—	12	23	40	16
Ar Control	68	—	22	10	—	—	—
AQ55 blank	72	—	—	20	7	—	—

3.4. The Effects of Power

In an initial experiment, both 10W and 50W powers were analyzed for a 5% O_2/10% Ar/90% CF_4 plasma after 1 minute of exposure. XPS spectra revealed an increase in the percent atomic fluorine from 9 % at 10W to 31% at 50W. This increase in fluorination was expected since higher powers enhance ion collisions, producing a greater concentration of active species in the plasma. A slightly higher O/C ratio resulted with increased power. Further experiments were designed to analyze the affects of power on the type and degree of modification. Since a 10 W plasma could not be sustained reproducibly, a 20 W 10% Ar/90% CF_4 plasma was used. Since the previous experiments conclusively show that the presence of the quartz plate was necessary to minimize degradation and etching, and maximize fluorination, the following experiments were conducted with the quartz plate present.

Contact angles measured on the surface of AQ55 after the 20W, Ar/CF_4 plasma modification are plotted in Figure 36 as a function of exposure time. The sessile drop contact angles increase at a more rapid rate for the 20 W exposure in comparison to the 50 W exposure (Figure 28 page 70) under the same conditions. Equilibrium contact angles are similar for both 50 W and 20 W plasma exposures. From the contact angle measurements, power does not appear to have a significant affect on surface fluorination.

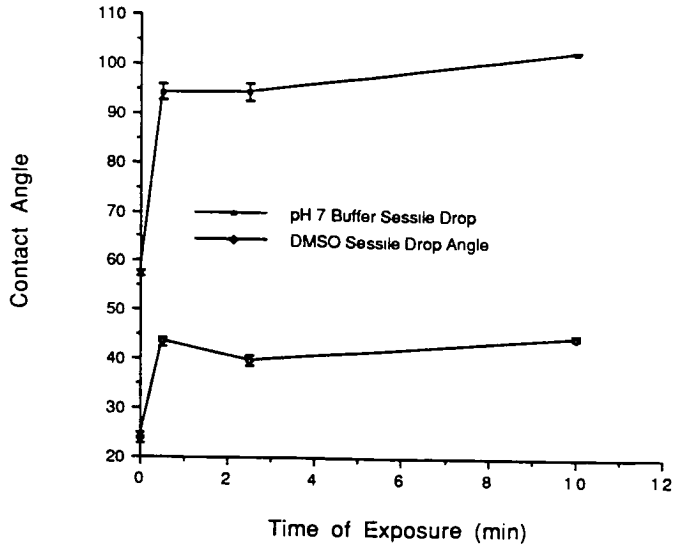

a)

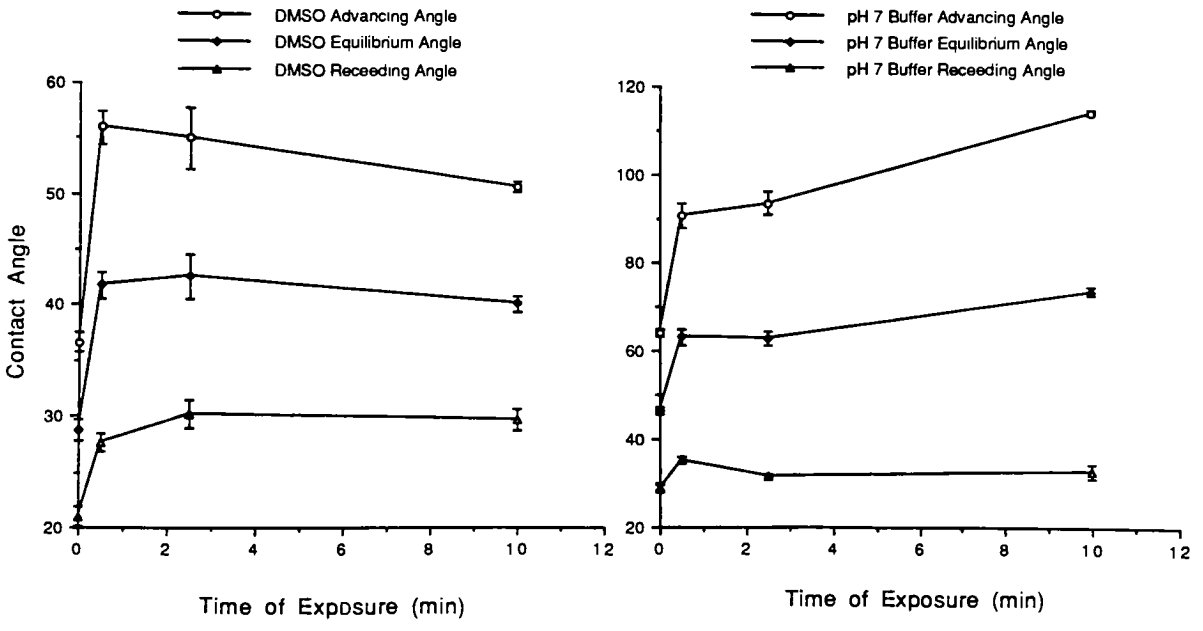

b) c)

Figure 36: Contact angles were measured on the surface of AQ55 after exposure to a 20 W, 10% Ar/90% CF_4 plasma. a)Sessile drop contact angles and advancing, receding, and equilibrium contact angles are plotted as a function of exposure time for both b) DMSO and c) pH 7 buffer contacting solvents.

The SEM micrographs for the surface of AQ55 after exposure to a 20W, 10% Ar/90% CF_4 plasma are shown in Figure 37. The micrographs show no change in surface topography after exposure to a 50 W, Ar/CF_4 plasma while protected by the quartz plate. Once again, the quartz plate was a vital in eliminating surface damage caused by ion bombardment even at long exposure times.

Temperatures measured after the 20 W plasma were not as high as those measured for the corresponding 50 W plasma. This suggests that the temperature may be dependent upon the power applied to the cathode. Power affects the energy of the plasma directly, therefore it should directly affect the plasma temperature at constant pressure and volume. A plot of the temperature as a function of exposure time is shown in Figure 38. The temperatures remain near the glass transition temperature of AQ55 from a low of 47^{o} C after 30 seconds to a high of 58^{o}C for both 2.5 and 10 minute exposures. Longer exposure times allow for the temperature to equilibrate, therefore temperatures were expected to increase with time. As a result of the lower temperature, reaction rates would also be expected to decrease. Therefore, the rate of fluorination, degradation and depropagation would decrease. This was shown to have occurred by the XPS data. Between 2.5 and 10 minutes, the percent atomic fluorine reached an average of 58% after a 50 W exposure when the 20 W exposure resulted in an average of 48% atomic fluorine. The C 1s spectrum for the 20 W exposures do not show as rapid of a shift to higher binding energy with time of exposure as the 50 W C 1s peaks (Figure 34, page 78). This indicates that fluorination did not occur into the depth of the AQ55 surface as rapidly as for the higher powers.

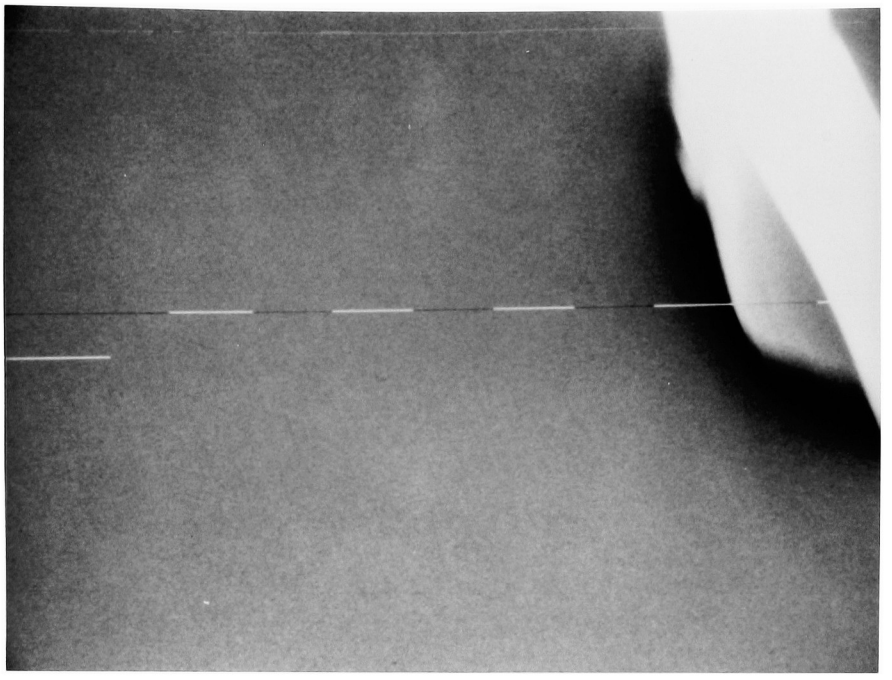

a) AQ55 after a 2.5 minute plasma exposure at 10,000 x.

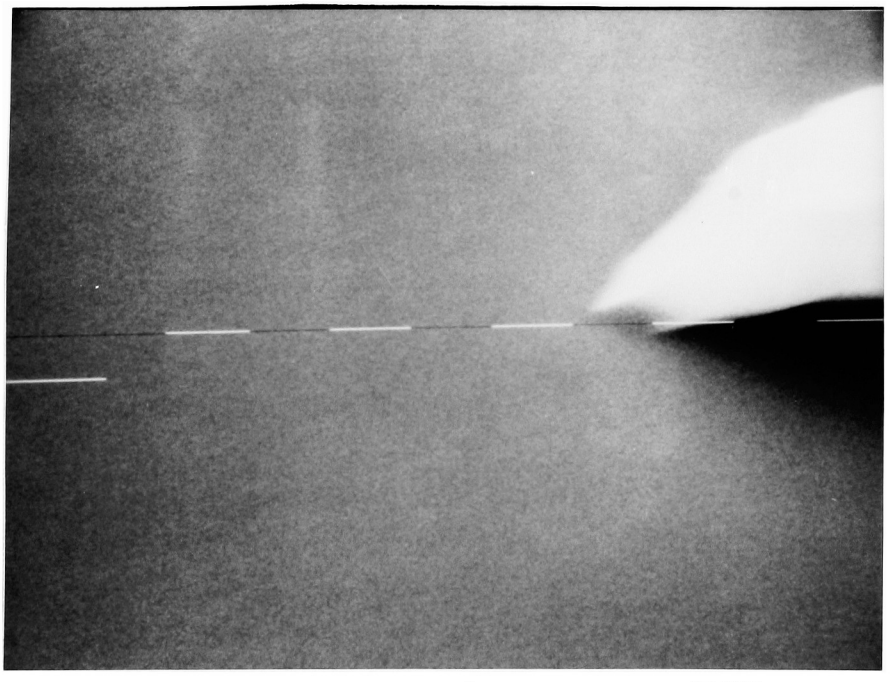

b) AQ55 after a 10 minute plasma exposure at 10,000 x.

Figure 37: SEM micrographs for AQ55 surfaces after exposure to a 20W, 10% Ar/90% CF_4 plasma for a) 2.5 minutes, and b) 10 minutes.

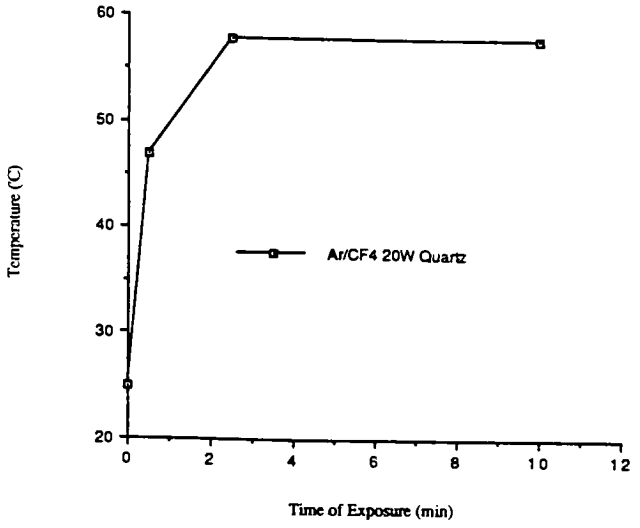

Figure 38: A plot of temperatures as a function of exposure time for 20 W, 10% Ar/90% CF_4 plasmas.

Gravimetric analysis revealed no significant weight changes for AQ55 samples exposed to the 20 W plasma. The absence of any weight loss indicates that etching and/or water evolution was not occurring to a significant degree.

FTIR/MIR analysis of AQ55 membranes exposed to the 20 W, Ar/CF_4 plasma did not reveal any changes in chemical functionalities at the AQ55 surface after all three exposure times. This indicates that the 20 W plasma may have been the mildest plasma exposure the AQ55 samples were subjected to. Any modification that did occur as a result of the 20 W plasma exposure only affected a thin layer of the AQ55 surface, approximately < 50 Å, and could not be detected by FTIR/MIR analysis.

Atomic percents of carbon, oxygen, and fluorine detected at the surface of AQ55 after exposure to the 20W plasma are shown as a function of exposure time in Figure 39. Sodium was not detected at the surface after all three exposures indicating that degradation of the surface did not occur under these plasma conditions.

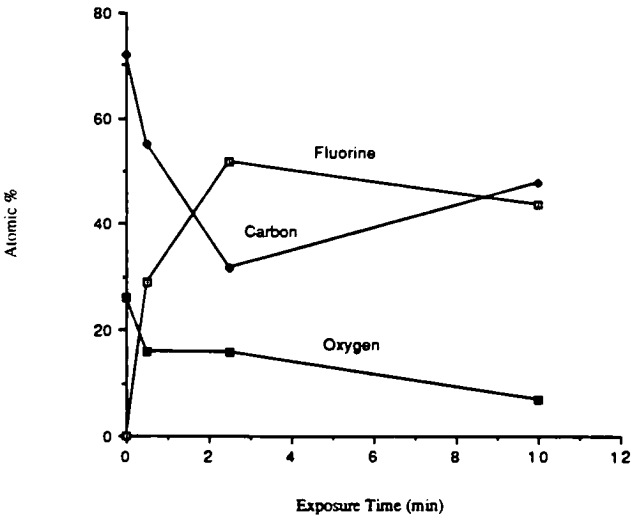

Figure 39: The atomic percents carbon, oxygen, and fluorine detected on the surface of AQ55 after exposure to a 20W, 10% Ar/ 90% CF_4 plasma protected by a quartz plate. Atomic percents are plotted as a function of exposure time.

The O/C ratios are plotted in Figure 40 as a function of exposure time for the 20 W plasma exposure. The O/C ratio does not appear to follow any apparent pattern. As fluorination increases, it was expected that the O/C ratio would decrease as the result of the grafting of CF_X species to the surface.

However that is not the case here. After 2.5 minutes of exposure, the atomic percent fluorine increased to 52%, however, the O/C ratio also increased to 0.49. The results suggest that the plasma conditions did not produce enough energy to effectively surmount the activation energy of fluorination and oxidation. As a result the probability of completing each initiated reaction is low, and the results appear random.

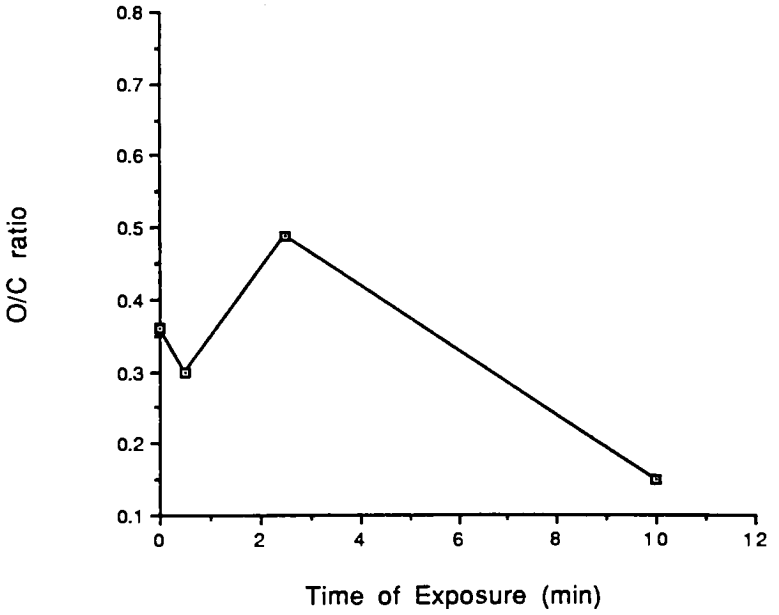

Figure 40: The O/C ratio at the surface of AQ55 a function of exposure time. AQ55 samples exposed to a 20 W , 10%Ar/90% CF_4 plasma while under a quartz plate.

C 1s spectra for AQ55 samples exposed to a 20 W, 10% Ar/ 90% CF_4 plasma are shown in Figure 41. The percent contribution of each of the

carbon peaks and the assigned carbon-oxygen and/or carbon-fluorine functionalities are listed in Table 11. The C 1 s spectrum looks very similar to those for the unmodified AQ55 and the Ar plasma control spectrum after 30 seconds exposure to the 20 W plasma. A significant shift to higher binding energies was not observed until after 10 minutes of exposure. When comparing the C 1s spectra as a function of power (C 1s spectra for 50 W exposures shown in Figure 34, page 78), a much slower shift to higher binding energies was observed at the lower power. Also a higher percent of CF_3 functionalities were observed at higher powers. Therefore, in order to maximize fluorination, the 50 W plasma would be more favorable.

Table 11: The binding energy, percent contribution, and the assigned carbon-oxygen and carbon-fluorine functionalities for each of the contributing C1s peaks for the 20W, Ar/CF_4 plasma modified AQ55 surfaces. Samples were placed beneath the quartz plate during plasma exposure.

Exposure Time (min)	282 -284 eV % CH_2	285 -286 eV %C-CO %C_nF	287 eV % C-O %C_nF	287 eV %C-O %C_nF	289 eV %C=O %C_nF	291 eV %COO^- %C-CF_2	292 eV %CF_3
0.5	73	—	18	6	—	—	—
2.5	46	19	—	13	6	6	3
10	—	22	—	20	27	24	7
AQ55 Blank	72	—	—	20	7	—	—

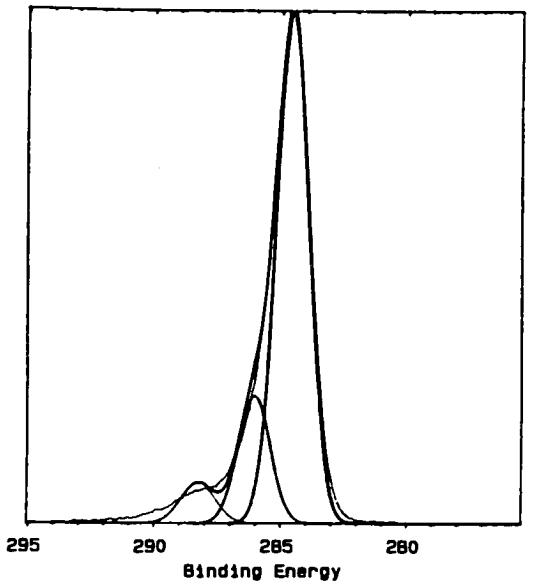

a)

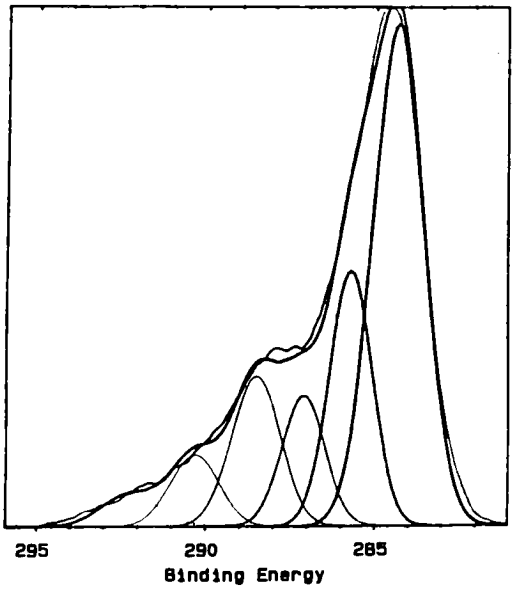

b)

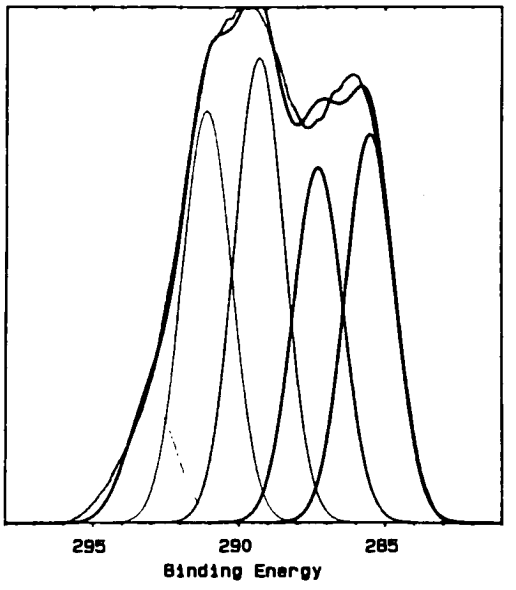

c)

Figure 41: C 1s spectra for the AQ55 surfaces exposed to a 20W, 10% Ar/90% CF_4 plasma while under the quartz plate for a) 0.5 minutes, b) 2.5 minutes, and c) 10 minutes.

4.0. Conclusion

The effect of variations in plasma parameters on the fluorination, degradation, and etching of poly(ester sulfonic) acid anionomeric membranes was examined. The objective of this thesis was to determine how the plasma gas composition, power, placement of the sample, and time of exposure could be used to maximize surface fluorination and minimize degradation of polymer films. Various levels of fluorination were achieved for all the plasma conditions examined. However, the key factor which maximized surface fluorination was the elimination of surface degradation and etching by alterations of the plasma parameters. Three factors which were found to promote surface degradation and etching included; the presence of oxygen in the gas feed, high energy ion bombardment, and increases in the plasma temperature. However, regardless of the plasma parameters, surface degradation was found to increase with time of plasma exposure. Under conditions where degradation was minimized, the depth and degree of fluorination increased with time of exposure. Chronologically, the following discussion will include the effects of oxygen in the plasma, sample placement, and power.

The 50 W, 5% O_2/10% Ar/85% CF_4 plasma (no quartz plate) was found to increase surface energy, promote fluorination, oxidation, degradation, and etching of the AQ55 surface through contact angle, XPS and SEM analysis. Contact angles dropped beyond 2 minutes of exposure indicating an increase in the AQ55 surface energy with length of exposure. The XPS data supported this by showing an increase in the O/C ratio to 0.47 from 0.35 on an unmodified surface. This suggested that surface oxidation

contributed to the production of a higher surface energy through the formation of polar carbon-oxygen functionalities at the surface. SEM micrographs revealed extensive surface damage which intensified with time of exposure. This change in surface topography occurred at the same exposure time in which contact angles dropped. As a result, surface oxidation and the change in the surface topography were factors which increased the surface energy. A significant weight loss was observed after each exposure time. This was considered to be a result of two processes; the evolution of water and etching of the AQ55 surface. Etching would have caused an increase in the number of chain ends at the AQ55 surface thereby increasing the surface energy. However, there is not sufficient evidence that etching has occurred. An increase in the surface sodium content from 0% on the unmodified surface to 9% atomic sodium after $O_2/Ar/CF_4$ plasma exposure was also an indication of surface degradation and possibly etching. Portions of the surface were exposed either because of chemical etching or reformation of the surface through high energy ion bombardment at elevated temperatures. This realignment of sodium ions was more predominate when oxygen was present in the gas feed. Therefore, oxygen contributed significantly to surface degradation.

Approximately 30% atomic fluorine was achieved at the AQ55 surface after exposure to the 50 W, 5% O_2/10% Ar/85% CF_4 plasma (no quartz plate shield). However, the shift in the C 1s spectrum to higher binding energies was not observed. This indicates that a high degree of fluorination was not achieved within the depth of XPS analysis (~ 50Å). With oxygen present in the gas feed, fluorination rates dropped since reactive fluorine species had to

compete with atomic oxygen for sites on the AQ55 backbone. This correlates with the alkoxy degradation mechanism[17] proposed. Atomic oxygen has been shown in the literature to decrease the relative concentration of -CF_x fragments found in the plasma. This explains why grafting of CF_x fragments was not found and indicates that the fluorination found was dominated by the addition of F species. The FTIR/MIR fluorocarbon vibrational bands were not observed until after 5 minutes of $O_2/Ar/CF_4$ plasma exposure. The same absorption bands were observed after only 1 minute of exposure to the Ar/CF_4 plasma. These results indicate that the competition between active oxygen species for carbon sites aided in decreasing the penetration of fluorine into the depth of the surface.

Elimination of oxygen from the gas feed proved to decrease surface oxidation thereby decreasing the surface energy. Equilibrium contact angles increased after exposure to the 50 W, 10% Ar/90% CF_4 plasma (no quartz plate). This corresponded to the decrease in the O/C ratio from 0.35 to approximately 0.26 between 2.5 and 10 minutes of exposure. Changes in surface topography were similar for oxygen containing and non oxygen containing plasmas. This indicates that oxidation was a major factor in producing a higher surface energy for AQ55 samples exposed to the oxygen containing plasma. However, the change in surface topography was still a contributing factor to the variations in surface energy but was not caused oxidation alone.

XPS analysis of AQ55 surfaces exposed to the 50 W, 10% Ar/90% CF_4 plasma (no quartz plate) revealed 2% atomic sodium and an average of 25% atomic fluorine on the surface. The increase of approximately 2% atomic

sodium indicates some degradation of the surface had occurred. Conclusive evidence of surface degradation was demonstrated by the SEM micrographs. However, the sodium content increased 7% for modifications with oxygen containing plasmas, the increased damage was caused by the surface oxidation or ion bombardment of oxygen atoms/ions within the plasma. After removal of oxygen, the percent of atomic fluorine appears to go unchanged . Shifts in the C 1s peaks began at 30 seconds and 2.5 minutes of exposure, yet after a 10 minute exposure, the C 1s spectrum was similar to the blank C 1s spectrum. Without the protective quartz plate ion bombardment was significant. This aided in ion milling, and the formation of a new surface. This effect limited the depth of surface fluorination. As a result, C 1s peaks for exposures without the quartz plate have a significant contribution from hydrocarbon rather than fluorocarbon functionalities.

In order to decrease and hopefully eliminate the effects of high energy ion bombardment, a quartz plate shield was suspended above the samples during plasma exposure. The use of the quartz plate shield was found to double the percent atomic fluorine, decrease oxidation, and degradation relative to surface modified without the quartz plate shield. SEM micrographs did not show any change in surface topography even after an extended exposure of 30 minutes. Also, since sodium was not detected on any samples protected with the plate, significant degradation did not occur. The FTIR/MIR analysis also supports these results showing no loss in the carbon-oxygen functionalities. These results correlate with the results found by Egitto[20] when polyimide etch rates were significantly reduced through the use of a quartz shield.

A level of 58% atomic fluorine was achieved at the AQ55 surface after exposure to the 50 W, 10% Ar/90% CF_4 plasma with the quartz plate shield present. Only 25% atomic fluorine was achieved at the AQ55 surface after a similar plasma exposure without the quartz plate. Also, a larger shift in the C 1s binding energy was observed after plasma modification with the quartz plate shield. This indicates that there is a higher level of CF_x type bonding extending into the depth of the AQ55 surface as a result of the decreased ion bombardment. Since fluorination was allowed to progress, the O/C ratios dropped to a low of 0.05 because of the grafting of CF_x functionalities.

Changing the applied power from 50 W to 20 W resulted in slower rates of fluorination and degradation. No weight loss, or changes in surface topography are observed after the 20 W plasma exposure. Also, FTIR/MIR results show no change in surface functionalities. The 30 second exposure to the 50 W Ar/CF_4 plasma exposure (with the quartz plate shield) reached 56% atomic fluorine at the AQ55 surface as compared to only 29% atomic fluorine with the 20 W plasma. Also longer exposure times were required to observe a shift in the C 1s binding energy. Since the percent atomic fluorine and O/C ratios were sporadic and reaction rates were slow, it is believed that the 20 W power does not provide enough energy to overcome the activation energy for surface fluorination. Temperatures measured for the 20 W plasma were lower indicating that the plasma energy decreased. Increased temperatures measured for the 50 W plasma assist diffusion of fluorine into the surface by creating a larger void volume in the polymer matrix.

The reactivity of a polymer chain is known to increase above the Tg of the polymer. As a result, AQ55 was more susceptible to depropagation, chain

scissioning, oxidation and fluorination at the temperatures measured for higher power plasma experiments. Therefore, the increased temperatures are believed to be a third factor which increased the probability of oxidation, degradation and etching at the AQ55 surface.

The plasma conditions found to achieve a maximum in surface fluorination with minimal surface degradation of the AQ55 membrane are; a gas composition of 10% Ar/90% CF_4 at a 50 W power with the quartz plate shield present. Under these plasma conditions, the most significant shift in the C 1s peak to higher binding energies is observed. This shift in the C 1s peak was attributed to the addition of atomic fluorine to the carbons in the AQ55 backbone. Decreases in the C 1s peak attributed to the CH_X functionality indicate that a high conversion from CH_X to CF_X type functionality is achieved within the 50 Å depth of analysis. The level of fluorination achieved under these plasma conditions is found to be 60% atomic fluorine at a depth of 50 Å. Dramatic decreases in the O/C atomic ratio are also found indicating that oxidation is not occurring, rather, grafting of CF_X functionalities are taking place. SEM, gravimetric and FTIR/MIR analyses reveal no significant changes in surface topography, sample weight, and no loss in carbon-oxygen functionalities on the AQ55 surface. A smooth surface was observed in the SEM micrographs, even after 30 minutes of plasma exposure. Contact angle also showed a decrease in surface energy as a result of the fluorination.

The use of the quartz plate and elimination of oxygen from the gas feed proved to be the most critical parameter changes which aided in surface fluorination by limiting the effects of degradation and etching. Although

there is not conclusive evidence for etching, it is believed to be a significant part of the modification processes examined. The significant contributors for etching include oxygen, high energy ion bombardment, highly reactive radicals, and exposure to elevated temperatures. The primary mechanism for etching occurs through chain scissioning which is initiated by oxidation (alkoxy degradation), ion milling, and other radical reactions. Allowing chain scissioning reactions to progress, the possibility exists for the formation of low molecular weight fragments which can be removed from the membrane surface. These effects would be intensified with exposure to temperatures above the Tg of the polymer. As a result of etching processes, a new surface may have been continually reformed during exposure, thereby not allowing for the progression of fluorination to occur to a significant depth. Even after ion bombardment and oxygen were eliminated, the membrane was still exposed to reactive radicals, high temperatures and very possibly trace amounts of oxygen causing some etching to occur. Also, with the high temperature exposure, the surface was kept in a dynamic state allowing for the diffusion of active species into the matrix of the polymer. With this effect, chain scissioning and oxidation could occur within the surface depth as well. Therefore etching may have progressed from the surface into the bulk as well as from the bulk out. The same temperature effect is believed to have aided in the penetration of fluorine species, thereby increasing the depth of fluorination.

Appendix I

RCA Cleaning of Silicon Wafers

Procedure:

(1) Prepare a 1:1:5 mixture of $NH_4OH/H_2O_2/H_2O$. (30% unstabilized H_2O_2, 27% NH_4OH, deionized H_2O) Heat mixture to 70 to 80°C. Place silicon wafers into heated mixture for 10 to 20 minutes.

(2) Transfer silicon wafers to the water dump rinser. Rinse wafers with 4 cycles of deionized H_2O.

(3) Place wafers into a 1:10 mixture of HF/H_2O for 1 minute at room temperature.

(4) Transfer silicon wafers to the water dump rinser. Rinse wafers with 4 cycles of deionized H_2O.

(5) Place wafers into a 1:1:5 mixture of $HCl/H_2O_2/H_2O$. Heat mixture to 70 to 80°C for 10 to 20 minutes.

(6) Rinse wafers in the cascade rinser with deionized H_2O until the rinse water reached 18MΩ.

(7) Finally, spin the wafers dry.

References

(1) D.T. Clark, W.J. Feast, W. K.R. Musgrave, and I. Ritchie, *J.Polym. Sci., Polym. Chem. Ed.*, **13**, 857-890 (1975).

(2) M. Anand, R.E. Cohen, and R.F. Baddour, *Polymer*, **22**, 361-371 (1981).

(3) G.A. Corbin, R.E. Cohen, and R.F. Baddour, *Polymer*, **23**, 1546-1548 (1982).

(4) T. Yagi, A. E. Pavlath, and A.G. Pittman, *J. Appl. Polym. Sci.*, **27**, 4019-4028 (1982).

(5) G.A. Corbin, R.E. Cohen, and R.F. Baddour, *Macromol.*, **18 (1)**, 98-103 (1985).

(6) M. Strobel, S. Corn, C.S. Lyons, and G.A. Korba, *J. Polym. Sci., Polym. Chem. Ed.*, **23**, 1125-1135 (1985).

(7) M. Strobel, S. Corn, C.S. Lyons, and G.A. Korba, *J. Polym. Sci., Polym. Chem. Ed.*, **25**, 1295-1307 (1987).

(8) M. Strobel, S. Corn, C.S. Lyons, and G.A. Korba, *J. Polym. Sci., Polym. Chem. Ed.*, **25**, 3343-3348 (1987).

(9) V. Vukanovic, F.D. Egitto, F. Emmi, L.J. Matienzo, E. Matuszak and G.A. Takacs, in the Eighth International Symposium on Plasma Chemistry, Tokyo, Japan, Aug. 31 - Sept. 4, 1987.

(10) L.J. Matienzo, F. Emmi, F.D. Egitto, D.C. Van Hart, V. Vukanovic, and G.A. Takacs, *J Vac. Sci. Technol.*, **A6 (3)**, 950-953 (1988).

(11) M. Verreault, J.E. Klemberg-Sepieha, E. Sacher, and M.R. Wertheiemer, *Appl. Surf. Sci.*, **44**, 165-169 (1990).

(12) V. Vukanovic, G.A.Takacs, E.A. Matuszak, F.D. Egitto, F. Emmi, and R.S. Horwath, *J. Vac. Sci. Technol.*, **B6 (1)**, 66-71 (1988).

(13) R. d'Agostino, F. Cramarossa, and S. De Benedictis, *Plasma Chem. Plasma Process.*, **2 (3)**, 213-231 (1982).

(14) R. d'Agostino, F. Cramarossa, V. Colaprico, and R. d' Ettole, *J. Appl. Phys.*, **54 (3)**, 1284-1288 (1983).

(15) E.A. Truesdale and G. Smolinsky, *J. Appl. Phys.*, **50 (11)**, 6594-6599 (1979).

(16) N.J. Chou, J. Parazsczak, E. Babich, Y.S. Chaug, and R. Goldblatt, *Microelectronic Engineering*, **5**, 375-386 (1986).

(17) F.D. Egitto, V. Vukanovic, and G.N. Taylor in*Plasma Deposition, Treatment, and Etching of Polymers;* R. d'Agostino, Ed.; Academic: San Diego, 1990; Chapter 5.

(18) *Plasma Deposition, Treatment, and Etching of Polymers;* R. d'Agostino, Ed.; Academic: San Diego, 1990; Chapter 2.

(19) B.N. Chapman, *Glow Discharge Processes; Sputtering and Plasma Etching;* John Wiley and Sons; New York, 1980; Chapters 1 and 2.

(20) F.D. Egitto, F. Emmi, R.S. Horwath, and V. Vukanovic, *J. Vac. Sci. Technol.*, **B3 (3)** 893-904 (1985).

(21) K. Harada, *J. Appl. Polym. Sci.* , **26**, 1961-1973 (1981).

(22) M. Anand, R.E. Cohen, and R.F. Baddour, *Photon, Electron, and Ion Probes of Polymer Structure and Properties*, edited by D.W. Dwight, T.J. Fabish, and H. R. Thomas (ACS Symposium Series, American Chemical Society, Washington, D.C., 1981), Vol. 162.

(23) B. Lamontagne, A.M. Wrobel, G. Jabert, and M.R. Wertheimer, *J. Phys. D:* **20**, 844-850 (1987).

(24) J.G. Fagan, *Reactive Ion Etching of Polyimide Films Using a Radio Frequency Discharge*, Rochester Institute of Technology, Masters Thesis, 1987.

(25) A. Eisenburg, B. Hird, *Macromol.*, **25 (24)**, 6466-6474 (1992).

(26) A.W. Adamson, *Physical Chemistry of Surfaces, 4th Ed.* ; John Wiley and Sons; New York, 1982; Chapter 10.

(27) J.J. Bikerman, *Physical Surfaces;* Academic Press; New York, 1970; Chapter 6.

(28) *Contact Angle, Wettability, and Adhesion;* R.F. Gould, Ed. (ACS Symposium Series, American Chemical Society, Washington, D.C., 1964), Vol. 43, Chapters 1,4,7,23.